Carbon and hydrogen isotopic compositions of stratospheric methane: 2. Two-dimensional model results and implications for kinetic isotope effects

M. C. McCarthy,[1] K. A. Boering,[1,2] A. L. Rice,[3,4] S. C. Tyler,[5] P. Connell,[6] and E. Atlas[7]

Received 15 November 2002; revised 27 February 2003; accepted 4 April 2003; published 8 August 2003.

[1] New high-precision measurements of the carbon and hydrogen isotopic compositions of stratospheric CH_4 made on whole air samples collected aboard the NASA ER-2 aircraft are compared with results from the Lawrence Livermore National Laboratory 2-D model. Model runs incorporating sets of experimentally determined kinetic isotope effects (KIEs) for the reactions of CH_4 with each of the oxidants OH, $O(^1D)$, and Cl are examined with the goals of determining (1) how well the 2-D model can reproduce the observations for both the carbon and hydrogen isotopic compositions, (2) what factors are responsible for the observed increase in the apparent isotopic fractionation factors with decreasing methane mixing ratios, and (3) how sensitive the modeled isotopic compositions are to various experimentally determined KIEs. Bound by estimates of the effects of uncertainties in model chemistry and transport on isotopic compositions, we then examine the constraints the ER-2 observations place on values for the KIEs. For the carbon KIE for reaction of CH_4 with $O(^1D)$, for example, the analysis of model results and observations favors the larger of the experimental values, 1.013, over a value of 1.001. These analyses also suggest that intercomparisons of results from different models using a given set of KIEs may be useful as a new diagnostic of model-model differences in integrated chemistry and transport. *INDEX TERMS:* 0317 Atmospheric Composition and Structure: Chemical kinetic and photochemical properties; 0322 Atmospheric Composition and Structure: Constituent sources and sinks; 0341 Atmospheric Composition and Structure: Middle atmosphere—constituent transport and chemistry (3334); 0365 Atmospheric Composition and Structure: Troposphere—composition and chemistry; *KEYWORDS:* methane, stratospheric methane, methane isotopes, carbon isotopes, hydrogen isotopes

Citation: McCarthy, M. C., K. A. Boering, A. L. Rice, S. C. Tyler, P. Connell, and E. Atlas, Carbon and hydrogen isotopic compositions of stratospheric methane: 2. Two-dimensional model results and implications for kinetic isotope effects, *J. Geophys. Res.*, *108*(D15), 4461, doi:10.1029/2002JD003183, 2003.

1. Introduction

[2] Recent fluctuations in the growth rate of atmospheric methane are not well understood [e.g., *Simpson et al.*, 2002], despite numerous model assessments of its sources and sinks over the last decade [e.g., *Fung et al.*, 1991; *Hein and Crutzen*, 1997; *Houweling et al.*, 1999]. Without a quantitative understanding of how methane's sources and sinks have changed both in the last decade and over the past 200 years, extrapolating how the sources and sinks will respond to climatic changes in the future cannot be done with confidence. Since methane is a greenhouse gas that contributes about 20% of the enhanced radiative forcing relative to preindustrial times [*Shine et al.*, 1996], predictions of its atmospheric concentration are necessary to accurately model future global climate change. In addition to its role as a greenhouse gas, methane plays a major role in both tropospheric and stratospheric chemistry. In the troposphere, methane levels regulate the oxidative capacity of the atmosphere, while in the stratosphere methane is a precursor of the HO_x family of free radicals that control the balance of ozone.

[3] To reduce uncertainties in the global budget of CH_4, the carbon isotopic composition of tropospheric methane has been used as an additional constraint on the strengths and global distributions of the CH_4 sources and sinks. Various sources of CH_4 (e.g., animals, rice production, fossil fuels), exhibit a characteristic range of values for the ratio of ^{13}C to ^{12}C [or "$\delta^{13}C$" values, where $\delta^{13}C = [(^{13}C/^{12}C)_{sample}/(^{13}C/^{12}C)_{standard} - 1) * 1000$, which is

[1]Department of Chemistry, University of California, Berkeley, California, USA.
[2]Department of Earth and Planetary Science, University of California, Berkeley, and Earth Science Division, Lawrence Berkeley National Laboratory, Berkeley, California, USA.
[3]Department of Chemistry, University of California, Irvine, California, USA.
[4]Now at Joint Institute for the Study of the Atmosphere and Ocean, University of Washington, Seattle, Washington, USA.
[5]Department of Earth System Science, University of California, Irvine, California, USA.
[6]Atmospheric Sciences Division, Lawrence Livermore National Laboratory, Livermore, California, USA.
[7]Atmospheric Chemistry Division, National Center for Atmospheric Research, Boulder, Colorado, USA.

0148-0227/03/2002JD003183$09.00

expressed in parts per thousand or "per mil" ≡ ‰]. The gas-phase sinks - oxidation by OH radicals, electronically excited oxygen atoms ($O(^1D)$), and Cl atoms - also leave their imprint on the isotopic composition of atmospheric CH_4 since the reaction rate for the light isotopologue is faster than that for the heavy one, a phenomenon known as a kinetic isotope effect or "KIE." Thus, inverse modeling of observed CH_4 concentrations and isotopic compositions can be used to constrain the magnitude and distribution of individual sources [e.g., *Fung et al.*, 1991; *Hein and Crutzen*, 1997]. These modeling studies depend critically on the quality and range of atmospheric observations for both the mixing ratio and isotopic composition of CH_4. They also require accurate knowledge of the KIEs for the CH_4 sink reactions.

[4] Extensive observations of $\delta^{13}C$-CH_4 now exist in the troposphere [e.g., *Quay et al.*, 1999; *Tyler et al.*, 1999], and recent observations of δD-CH_4 [e.g., *Quay et al.*, 1999; *Rice et al.*, 2001] in the troposphere will enable additional constraints on CH_4 sources to the atmosphere to be obtained through modeling of tropospheric δD-CH_4. As atmospheric observations increase in number, time, and spatial distribution, uncertainties in the inverse model results due to undersampling of the atmosphere decrease. However, several studies have shown that uncertainties in experimental KIEs, or ignoring KIEs in sink reactions which were not thought to be important, can have a significant impact on predicted isotopic compositions and, therefore, on the modeled CH_4 budget. For example, the small difference between measured values for the carbon KIE for the CH_4 + OH reaction (1.0054 by *Cantrell et al.* [1990] versus 1.0039 by *Saueressig et al.* [2001]) alters the predicted $\delta^{13}C$-CH_4 in the free troposphere by ~1‰ [*McCarthy et al.*, 2001]; this change is comparable to the magnitude of the observed interhemispheric gradient in $\delta^{13}C$-CH_4 at the surface [*Quay et al.*, 1999]. Isotopic fractionation by reaction with Cl in the stratosphere and troposphere has also been shown to influence free tropospheric isotopic compositions [*Gupta et al.*, 1996; *Tyler et al.*, 1999; *McCarthy et al.*, 2001; *Wang et al.*, 2002]. Clearly, a better understanding of stratospheric fractionation processes and tests to determine the sensitivity of isotopic compositions to discrepancies in laboratory values for KIEs would help to identify uncertainties in the isotopic CH_4 budget.

[5] In this study, we compare the extensive set of new measurements of $\delta^{13}C$-CH_4 and δD-CH_4 on stratospheric CH_4 collected from the ER-2 aircraft [*Rice et al.*, 2003] with results from the Lawrence Livermore National Laboratory (LLNL) 2-D model. In the stratosphere, the isotopic compositions of CH_4 depend on the relative and absolute abundances of OH, Cl, and $O(^1D)$, KIEs for these sink reactions, and stratospheric transport. Despite this complexity, the ER-2 observations provide a new opportunity to investigate the roles of these three oxidants and their respective KIEs in determining the CH_4 isotopic compositions in a region of the atmosphere effectively isolated from both the soil sink and CH_4 sources at the Earth's surface. In Part 1, a chemistry-only Rayleigh box model was used to examine the relationship between the isotopic compositions of CH_4 and CH_4 mixing ratios as the relative fractions of oxidation by reaction with OH, Cl, and $O(^1D)$ were varied at a constant temperature of 225K. Here in Part 2, we use the LLNL 2-D model to expand on the analysis in Part 1 with a more realistic simulation of the chemical distributions, reaction rate coefficients, and transport and mixing in the stratosphere. First, we evaluate the overall performance of the LLNL 2-D model in simulating the ER-2 observations for both $\delta^{13}C$-CH_4 and δD-CH_4. Second, we examine different sets of experimental KIEs to determine the sensitivity of the modeled isotopic compositions to individual reactions with OH, Cl, and $O(^1D)$. Third, we test the interpretations of the observations from Part 1 beyond a simple Rayleigh framework using the 2-D model's chemistry and transport. We then analyze known or estimated errors in model chemistry and transport and estimate the effects of these model uncertainties on the isotopic compositions. Although no 2-D (or 3-D) model can perfectly simulate stratospheric chemistry and transport, we demonstrate that the simultaneous observations of both $\delta^{13}C$-CH_4 and δD-CH_4 provide a new "double constraint" on potential errors in model chemistry, model transport, and experimentally determined KIEs which is considerably more powerful than observations of either isotopic composition alone. Combining these estimates of model error and the double constraint of ER-2 observations for both $\delta^{13}C$-CH_4 and δD-CH_4, we then examine the discrepancies between and uncertainties in experimentally determined values for the KIEs for CH_4 oxidation. Finally, we briefly discuss how comparing the LLNL 2-D model results with both ER-2 observations and results from other models may be used as a new diagnostic for integrated chemistry and transport in the stratosphere.

2. Carbon and Hydrogen KIEs for CH_4 Oxidation

[6] Over the last 20 years, use of the carbon isotopic composition of CH_4 to quantify methane sources to the atmosphere has stimulated laboratory and theoretical studies of the KIEs for the CH_4 sink processes. Reaction with OH is responsible for 90 ± 5% of the total CH_4 sink in the troposphere; a soil sink accounts for the majority of the remaining 10 ± 5% [*Hein and Crutzen*, 1997]. Large carbon and hydrogen KIEs for the Cl sink measured since 1995 dictate that reaction with Cl atoms is an important factor in determining isotopic compositions in the stratosphere [e.g., *Gupta et al.*, 1996; *Bergamaschi et al.*, 1996; *Sugawara et al.*, 1997; *Tyler et al.*, 1999; *McCarthy et al.*, 2001; *Wang et al.*, 2002] where Cl atom concentrations are relatively high and the fraction of CH_4 oxidized by Cl is on the order of 20% (see section 4.1). However, the Cl sink may also be important in the troposphere, where the fraction of CH_4 oxidized by Cl may only be as high as ~1% [e.g., *Allan et al.*, 2001]. Thus, the tropospheric isotopic compositions are influenced by both in situ Cl oxidation as well as the return of heavy CH_4 from the stratosphere [e.g., *Gupta et al.*, 1996; *McCarthy et al.*, 2001; *Wang et al.*, 2002]. The third oxidant, $O(^1D)$, is responsible for approximately 25% of the stratospheric sink for CH_4 in the LLNL model (see section 4.1); thus, accurate KIEs for the reaction $CH_4 + O(^1D)$ are also necessary to predict stratospheric isotopic compositions.

[7] Recent experimental determinations of the carbon and hydrogen KIEs for the reactions of CH_4 with OH, Cl, and $O(^1D)$ are listed in Tables 1 and 2, respectively. For ease of

Table 1. Experimental Carbon KIEs

Reaction	Carbon KIE (k_{12}/k_{13})	Temperature Range, K	225 K	296 K	Reference
$OH + CH_4$	1.0054 ± 0.0009	273–353	1.0054	1.0054	*Cantrell et al.* [1990]
	1.0039 ± 0.0004	296	...	1.0039	*Saueressig et al.* [2001]
$Cl + CH_4$	1.043 * exp(6.455/T)	223–297	1.073	1.066	*Saueressig et al.* [1995]
	1.066 ± 0.002	296	...	1.066	*Crowley et al.* [1999]
	1.035 * exp(7.55 ± 1.64/T)	273–349	1.070	1.0621	*Tyler et al.* [2000]
$O(^1D) + CH_4$	1.001	298	...	1.001	*Davidson et al.* [1987]
	1.013	223–295	1.013	1.013	*Saueressig et al.* [2001]

comparison, values for the KIEs at room temperature and at a typical stratospheric temperature of 225 K are given in columns 4 and 5. KIEs with measured temperature dependences are plotted in Figure 1. Note that agreement at room temperature does not imply agreement at stratospheric temperatures. Before we investigate the sensitivity of the modeled isotopic compositions to differences in the experimentally determined KIEs, we first review the experiments used to determine the values for the KIEs listed in Tables 1 and 2. This review provides the experimental context for our analysis of results from different model scenarios used to evaluate discrepancies among these experimental KIEs. Theoretical calculations of the KIEs for CH_4 are quite challenging and appear to be very sensitive to the treatment of the potential energy surface for the reaction [*Corchado et al.*, 2000]; therefore, references to theoretical work are included below for completeness but are not discussed.

2.1. Carbon KIEs

2.1.1. CH_4 + OH

[8] The carbon kinetic isotope effect for the reaction of CH_4 with OH has been the focus of a number of laboratory [*Rust and Stevens*, 1980; *Davidson et al.*, 1987; *Cantrell et al.*, 1990; *Saueressig et al.*, 2001] and theoretical [*Melissas and Truhlar*, 1993; *Lasaga and Gibbs*, 1991; *Gupta et al.*, 1997; *Espinosa-Garcia and Corchado*, 2000] studies. The two most recent experimental determinations yielded values of 1.0054 ± 0.0009(2σ) [*Cantrell et al.*, 1990] and 1.0039 ± 0.0004(2σ) [*Saueressig et al.*, 2001]. The Cantrell experiment combined gas chromatograph-flame ionization detection (GC-FID) to measure CH_4 mixing ratios and dual-inlet isotope-ratio mass spectrometry (IRMS) to measure $\delta^{13}C$-CH_4 after exposure to OH over the temperature range 273–353 K. The source of OH in the experiment was $O(^1D) + H_2O$. Because $O(^1D)$ also reacts with CH_4, potential interference from $O(^1D)$ was monitored by measuring N_2O, which also reacts with $O(^1D)$. Because N_2O remained constant throughout the experiment to within the uncertainty of the N_2O measurements (i.e., N_2O remained at 98 ± 5% of its initial concentration), interference of $O(^1D)$ in the determination of the OH KIE was thought to be negligible. The Cantrell KIE has been used in the majority of both stratospheric and inverse modeling studies to date.

[9] Recently, *Saueressig et al.* [2001] combined GC-FID and IRMS measurements of CH_4 and $\delta^{13}C$-CH_4, respectively, to determine a value for the OH KIE at 296 K. In contrast to the Cantrell experiment, OH was generated from the photolysis of H_2O_2 with a Hg/Xe short arc lamp. The value for the KIE of 1.0039 ± 0.0004 was found to be independent of both bath gas (He/O_2 or N_2/O_2) and wavelength filter (280 or 225 nm), which indicated that an interfering reaction with $O(^1D)$ was unlikely to be significant. A second set of measurements reported in *Saueressig et al.* [2001] using HNO_3 as the OH source yielded more erratic values for the KIE between 1.0041 to 1.0055. While these latter values are closer to the results of the Cantrell experiment, they were considered by Saueressig et al. to be less reliable due to the presence of photo-labile secondary reaction products from the HNO_3 OH source.

[10] Importantly, the small but significant difference between the two most recently determined KIEs has yet to be resolved. Although the carbon OH KIE from these two studies yielded values that are relatively close, the range in their experimental uncertainties do not overlap, and this small difference in the measured KIE results in a significant change in predicted $\delta^{13}C$-CH_4 values in the free troposphere [*McCarthy et al.*, 2001]. Moreover, the KIE for OH is expected to depend on temperature [*Gupta et al.*, 1997] but has not yet been determined at temperatures of importance in many regions of the stratosphere.

2.1.2. CH_4 + Cl

[11] The surprisingly large carbon kinetic isotope effect for the reaction of CH_4 with Cl measured by *Saueressig et al.* [1995] stimulated a number of additional experimental [*Crowley et al.*, 1999; *Tyler et al.*, 2000] and theoretical [*Tanaka et al.*, 1996; *Gupta et al.*, 1997; *Roberto-Neto et al.*, 1998; *Corchado et al.*, 2000] studies over the past 7 years. Although initial theoretical studies showed marked

Table 2. Experimental Hydrogen KIEs

Reaction	Hydrogen KIE (k_H/k_D)	Temperature Range, K	225 K	296 K	Reference
$OH + CH_4$	0.91 * exp(75 ± 118/T)	293–361	1.27	1.16	*DeMore* [1993]
	1.09 * exp(49 ± 22/T)	249–422	1.36	1.25	*Gierczak et al.* [1997]
	1.294 ± 0.018	296	...	1.294	*Saueressig et al.* [2001]
$Cl + CH_4$	1.278 * exp(51.3 ± 19.1/T)	223–296	1.61	1.508	*Saueressig et al.* [1996]
	0.894 * exp(145 ± 42/T)	273–349	1.70	1.474	*Tyler et al.* [2000],
	1.47 ± 0.09	295	...	1.47	*Wallington and Hurley* [1992][a]
	1.54 ± 0.04	298	...	1.54	*Boone et al.* [2001]
$O(^1D) + CH_4$	1.06	223–295	1.06	1.06	*Saueressig et al.* [2001]

[a]Revised as quoted by *Saueressig et al.* [1996].

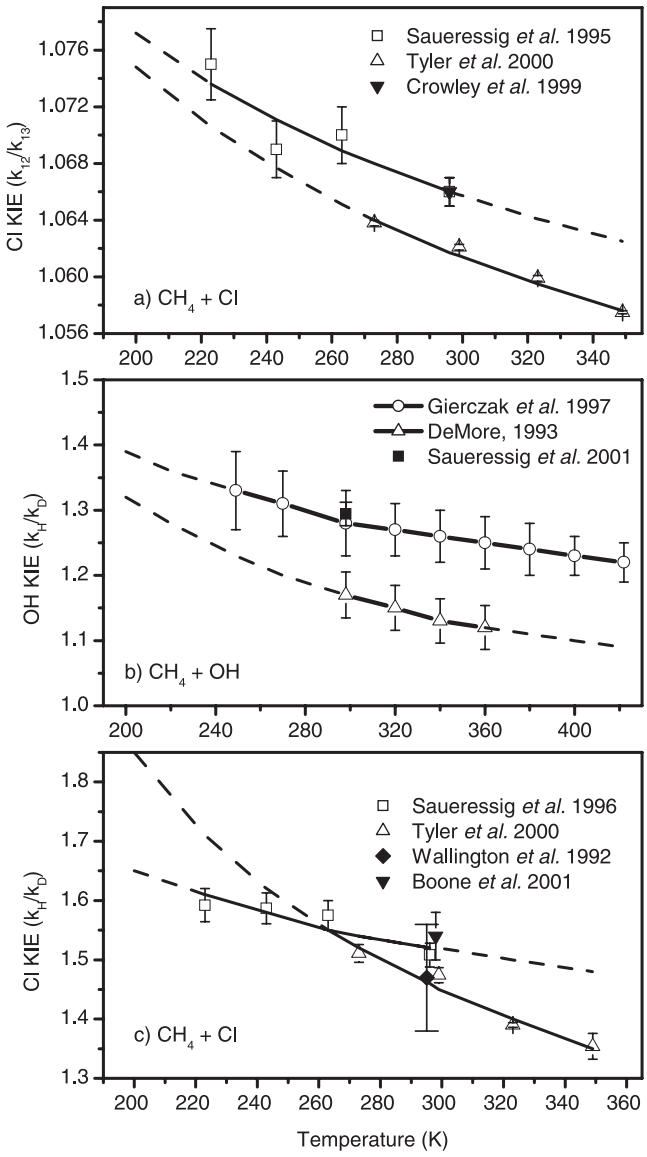

Figure 1. Experimentally determined kinetic isotope effects (KIEs) as a function of temperature for (a) the carbon KIE for CH_4 + Cl, (b) the hydrogen KIE for CH_4 + OH, and (c) the hydrogen KIE for CH_4 + Cl. Solid lines indicate the fit to the temperature dependence over the range of the experimental data, while dashed lines are an extrapolation of that fit to higher and lower temperatures. Error bars indicate the 1σ uncertainty.

disagreement with experiment, most recent work converges on a value for the Cl KIE of ~1.06 at 296 K. Experimental Cl KIEs are summarized in Table 1 and their temperature dependence is plotted in Figure 1a. *Saueressig et al.* [1995] used tunable diode laser absorption spectroscopy (TDLAS) to measure the ratio $^{12}CH_4/^{13}CH_4$ (using weak/strong line pairs for $^{12}CH_4/^{13}CH_4$ isotopologues) and GC-FID to measure CH_4 from 223 to 297 K. A follow-up experiment [*Crowley et al.*, 1999] using Fourier transform infrared spectroscopy (FTIR) to monitor the $^{12}CH_4/^{13}CH_4$ ratio in an isotopically enriched sample at room temperature yielded a similar result. Most recently, *Tyler et al.* [2000] used dual-inlet IRMS and GC-FID to monitor $\delta^{13}C$-CH_4 and CH_4 mixing ratios, respectively, to determine the Cl KIE from 273 to 353K. The differences between the experimental values for the Cl KIE are small relative to the size of the Cl KIE itself, which also suggests that this KIE is relatively well constrained compared to the OH KIE.

2.1.3. CH_4 + $O(^1D)$

[12] Far fewer studies of the carbon KIE for reaction of CH_4 with $O(^1D)$ have been performed than for OH and Cl. Due to its nearly collision rate-limited rate coefficient, theory predicts that this reaction should have a small KIE near unity [*Kaye*, 1987]. In an early experiment to measure the OH KIE using GC-FID and dual-inlet IRMS, *Davidson et al.* [1987] dedicated one trial run to CH_4 + $O(^1D)$ and measured a KIE for $O(^1D)$ of 1.001 at 298 K. A more recent experiment by *Saueressig et al.* [2001] using GC-FID and dual-inlet IRMS yielded a KIE for $O(^1D)$ of 1.013 - an order of magnitude larger than that of *Davidson et al.* [1987]. In this more recent experiment, a photochemical model was used to correct for an estimated 20 to 30% systematic error due to reaction with OH that is generated when $O(^1D)$ reacts with CH_4.

2.2. Hydrogen KIEs

2.2.1. CH_4 + OH

[13] The hydrogen kinetic isotope effect for the reaction of CH_4 with OH has been studied both experimentally [*Gordon and Mulac*, 1975; *DeMore*, 1993; *Gierczak et al.*, 1997; *Saueressig et al.*, 2001] and theoretically [*Melissas and Truhlar*, 1993; *Espinosa-Garcia and Corchado*, 2000]. The three most recent measurements of the OH KIE are listed in Table 2. *Gierczak et al.* [1997] used pulsed laser photolysis to produce OH and laser-induced fluorescence to detect the OH decay in order to measure absolute rates of reaction for CH_4 and CH_3D from 249 to 422 K. *DeMore* [1993] used a transfer standard method which determined the relative rates of reaction for CH_4 and CH_3D against the known standards HFC-134a and HCFC-141b from 293 to 361K. DeMore chose the HFC-134 data as yielding the more reliable KIE since there was less experimental scatter than for the HCFC-141b data. To within the 2σ experimental uncertainties, the two KIEs from the transfer-standard method of DeMore agree with each other and with the Gierczak KIE at 298 K. However, the DeMore KIE does not overlap within its 2σ uncertainty with a recent room temperature result reported by *Saueressig et al.* [2001] which used TDLAS and GC-FID to measure a KIE of 1.294 ± 0.018. Thus, the Gierczak KIE is within 2σ of both the DeMore and the Saueressig OH KIEs, but the DeMore and the Saueressig results are outside the bounds of their respective 2σ uncertainties.

2.2.2. CH_4 + Cl

[14] The hydrogen KIE for the reaction of CH_4 with Cl has also been the subject of recent laboratory [*Wallington and Hurley*, 1992; *Saueressig et al.*, 1996; *Tyler et al.*, 2000; *Boone et al.*, 2001] and theoretical [*Roberto-Neto et al.*, 1998; *Corchado et al.*, 2000] studies. Analogous to the carbon KIEs, the hydrogen KIE for reaction with Cl is considerably larger than that for OH, although only by a factor of 2 to 3 rather than the order of magnitude difference for carbon isotopic substitution. Experiments by *Saueressig et al.* [1996], *Tyler et al.* [2000], and *Boone et al.* [2001]

measuring relative rates yielded values for the Cl KIE at room temperature of 1.508 ± 0.041, 1.474 ± 0.020, and 1.54 ± 0.04, respectively. *Saueressig et al.* [1996] used TDLAS and GC-FID from 223 to 296K, *Tyler et al.* [2000] used dual-inlet IRMS with GC-FID from 273 to 349K, and *Boone et al.* [2001] used long-path FTIR at 298K. Earlier work by *Wallington and Hurley* [1992] using FTIR at 295K yielded a value of 1.36 ± 0.04, notably smaller than the more recent studies; however, upon additional measurements, they revised their KIE to 1.47 ± 0.09 (as noted by *Saueressig et al.* [1996] as a personal communication by T. J. Wallington). Thus, all experimental studies are in relatively good agreement at 296 K. The Saueressig and Tyler experiments show that the KIE increases with decreasing temperature (Figure 1c); the Tyler KIE has a stronger temperature dependence, with correspondingly higher values for the KIE when their temperature dependence is extrapolated below 260 K.

2.2.3. $CH_4 + O(^1D)$

[15] The hydrogen KIE for the reaction of CH_4 with $O(^1D)$ has received considerably less attention than those for OH and Cl. This KIE was until recently assumed to be near unity [e.g., *Kaye*, 1987] due to the nearly collision-limited rate coefficient for $CH_4 + O(^1D)$. However, a value of 1.06 from 223 to 295 K was recently reported by *Saueressig et al.* [2001]. The experiment used the TDLAS/GC-FID combination described above for the carbon $O(^1D)$ KIE experiment; as above, a correction based on a photochemical model was applied for interference from OH.

3. Two-Dimensional Modeling

[16] In order to analyze the ER-2 observations in a framework beyond the simple Rayleigh fractionation model of Part 1, we use the LLNL 2-D model to test the sensitivity of modeled isotopic compositions to different values of the KIEs discussed in section 2. Sets of isotope-specific rate coefficients for the reactions of $^{12}CH_4$, $^{13}CH_4$, and $^{12}CH_3D$ with OH, Cl, and $O(^1D)$ from Tables 1 and 2 were incorporated into the LLNL 2-D model. This two-dimensional chemical-radiative-transport model calculates zonally averaged distributions of chemically active trace species in the troposphere and stratosphere and has been used in numerous ozone assessment studies [e.g., *Kinnison et al.*, 1994; *World Meteorological Organization* (*WMO*), 1999] and one previous CH_4 isotope study [*McCarthy et al.*, 2001]. The processes represented include (a) thermal kinetic chemical reactions with rate constants based on climatological zonal temperature distributions, (b) photolytic chemical reactions, (c) advection and diffusion driven by climatological zonal average temperature, radiative transfer of energy, and orographic forcing, (d) surface emission and in situ production of active trace constituents, and (e) removal of active species by dry and wet deposition. The model domain extends from pole to pole and from the surface to 85 km. The horizontal resolution is 5° in latitude, and the vertical coordinate is logarithmic in pressure with an approximate resolution of 1.5 km. For this application, the model treats 63 chemically active species, including the isotopologues of CH_4, in 188 photochemical reactions using individual reactions rather than treatment as chemical families. Atomic Cl concentrations were simulated using a 1990 chemical inventories emission set; current CFC levels are about 10% higher [*WMO*, 1999]. Absolute reaction rate coefficients were taken from Jet Propulsion Laboratory reports JPL-97 and JPL-00 [*DeMore et al.*, 1997, 2000], with the exception of OH + CH_4, which was taken from *Gierczak et al.* [1997]. Use of this slightly larger rate coefficient decreased OH concentrations by <1% for most of the stratosphere and had a negligible effect on modeled CH_4 isotopic compositions in this study. Absolute reaction rate coefficients for the isotopologues $^{13}CH_4$ and $^{12}CH_3D$ were calculated as the rate coefficients for CH_4 divided by the appropriate KIE. Model numerics are such that the individual isotopologues of CH_4 can be modeled to a relative precision of better than 0.1‰.

[17] For this study, model scenarios using groups of carbon or hydrogen KIEs for each of the OH, Cl, and $O(^1D)$ oxidants were run; these model scenarios are listed in Tables 3 and 4. Scenarios C_S1 and D_S1 are arbitrarily assigned as the baseline scenarios for the carbon and hydrogen isotopic compositions respectively. The KIEs in the baseline scenarios were chosen on the basis of whether measurements of the KIE were made at temperatures relevant to the stratosphere (if available). The additional model scenarios use an alternate KIE from Table 1 or 2 such that the set of scenarios provides a means to assess the influence of each KIE on predicted isotopic compositions in the stratosphere.

[18] Boundary conditions were the same for all model scenarios: $^{12}CH_4$, $^{13}CH_4$, and $^{12}CH_3D$ at the surface were prescribed to reproduce the global average mixing ratio of 1750 ppbv in 1997 [e.g., *Dlugokencky et al.*, 2001] and observed values of −47.3‰ and −90.0‰ for $\delta^{13}C\text{-}CH_4$ and $\delta D\text{-}CH_4$, respectively, from the ER-2 observations in the troposphere [*Rice et al.*, 2003]. Each scenario was then run until $\delta^{13}C\text{-}CH_4$ and $\delta D\text{-}CH_4$ had converged to steady state to within ±0.01‰ and ±0.1‰, respectively, for all grid cells. Note that our goal here was to predict stratospheric isotopic compositions. Thus, as long as air entering the model stratosphere had values for CH_4, $\delta^{13}C\text{-}CH_4$ and $\delta D\text{-}CH_4$ that simulated the observations, it was not necessary to include realistic latitude-dependent CH_4 source fluxes nor to include the surface soil sink for CH_4 and its KIE. To test these assumptions, a number of sensitivity tests to surface conditions were run. A more realistic, latitude-dependent surface boundary condition for $\delta^{13}C\text{-}CH_4$, for example, was

Table 3. Model Scenarios for the Carbon KIEs

Scenario	OH KIE	Cl KIE	$O(^1D)$ KIE
C_S1	1.0054	1.043 * exp(6.455/T)	1.013
C_S2	1.0054	1.043 * exp(6.455/T)	1.001
C_S3	1.0039	1.043 * exp(6.455/T)	1.013
C_S4	1.0054	1.035 * exp(7.55/T)	1.013

Table 4. Model Scenarios for the Hydrogen KIEs

Scenario	OH KIE	Cl KIE	$O(^1D)$ KIE
D_S1	1.09 * exp(49/T)	1.278 * exp(51.3/T)	1.06
D_S2	1.09 * exp(49/T)	1.278 * exp(51.3/T)	1
D_S3	1.09 * exp(38/T)	1.278 * exp(51.3/T)	1.06
D_S4	1.09 * exp(49/T)	1.278 * exp(32.2/T)	1.06
D_S5	0.91 * exp(75/T)	1.278 * exp(51.3/T)	1.06

found to have little effect on the stratospheric isotopic composition, as expected from the simple eddy-diffusion-dominated tropospheric transport in the model. Changing the boundary condition for δ^{13}C-CH_4 at the surface from −47.0 to −47.5‰ had a negligible effect on the stratospheric δ^{13}C:CH_4 relationship beyond a constant offset of 0.5‰. Changing the surface boundary condition for the CH_4 mixing ratio between 1700 ppbv to 1800 ppbv also had little effect on the modeled δ^{13}C:CH_4 relationship except at low mixing ratios. However, since the stratospheric boundary condition is essentially the same as the global average tropospheric value and is known to better than ±15 ppbv [e.g., *Hurst et al.*, 1999; *Dlugokencky et al.*, 2001], we consider the impact of this sensitivity to be negligible. To test the validity of our steady state approach discussed earlier, a model run using a 30-year surface flux of δD-CH_4 values and CH_4 mixing ratios from the years 1970 to 2000 [*Braunlich et al.*, 2001] was also examined; CH_4, CFCs, and N_2O were set to vary with time. This model run yielded a δD-CH_4 relationship in the stratosphere that was within 2‰ of the steady state run that used the same KIEs, a difference which is smaller than the estimated 2σ error for the δD-CH_4 measurements. These results indicate that the steady state treatment using prescribed surface boundary conditions to reproduce current free tropospheric observations is a reasonable approximation for modeling the δ^{13}C:CH_4 and δD:CH_4 relationships in the stratosphere.

[19] In addition to the magnitudes of the KIEs and the values for the CH_4 mixing ratios and isotopic compositions for air entering the stratosphere, chemistry and transport are also important in determining δ^{13}C-CH_4 and δD-CH_4 in the stratosphere. Each of these is discussed separately in the following two sections.

3.1. Model Chemistry and Isotopic Compositions

[20] Predicted CH_4 isotopic compositions can be sensitive to both absolute and relative mixing ratios of the OH, Cl, and $O(^1D)$ radicals as well as to the absolute rates of chemical reactions used in the model. As an example of possible model sensitivity to absolute rates, *Wang et al.* [2002] in the Harvard 2-D model used a modified rate coefficient, suggested by *Michelsen et al.* [1996], for the reaction of CH_4 with Cl which is 5 to 30% larger than the JPL recommendation. Use of this larger rate coefficient resulted in an increase of about 0.5‰ in predicted δ^{13}C-CH_4 values for a given CH_4 mixing ratio in their model. Similarly, when Wang et al. increased Cl concentrations by a factor of 2 to match observations in the lower stratosphere, modeled δ^{13}C-CH_4 increased by a maximum of ∼2‰ at a CH_4 mixing ratio of 900 ppbv. Their model sensitivities illustrate that, to zeroth order, isotopic compositions can be equally sensitive to errors in oxidant concentration or kinetic rate coefficients for reaction with that oxidant. For example, increasing the reaction rate coefficient for CH_4 + OH by 25% is approximately equivalent to increasing the concentration of OH by 25% (e.g., $\{1.25 * k_{OH}\} * [OH] \cong k_{OH} * \{1.25 * [OH]\}$). Predicted isotopic compositions are also sensitive to the relative fractions of CH_4 oxidized by OH, Cl, and $O(^1D)$. We discuss this sensitivity in detail in section 4.4 below. We note here, however, that even if large changes are made in the absolute modeled radical abundances, there may only be a small corresponding change in the predicted isotopic composition if the relative fractions of CH_4 oxidized by each radical remain approximately the same. For example, an increase in Cl by a factor of 1.5 and OH by a factor of 2 in the Harvard 2-D model lower stratosphere resulted in only slightly heavier δ^{13}C-CH_4 (∼0.5‰ for CH_4 mixing ratios <1200 ppbv) than their baseline run [*Wang et al.*, 2002].

[21] Since the predicted isotopic compositions are sensitive to model chemistry, as *Wang et al.* [2002] showed using the Harvard 2-D model, we compare the LLNL 2-D model abundances of Cl, OH, and $O(^1D)$ to observations or proxies of radical mixing ratios in the stratosphere. The LLNL 2-D model simulates these radicals using the fundamental JPL recommended chemistry; therefore, it is not possible to "tune" the model to "match" observations. Comparisons with other models and measurements of stratospheric radical abundances show that the LLNL model does as well as the bulk of other models; no 2-D or 3-D model performs dramatically better [*Park et al.*, 1999]. Specifically, the LLNL 2-D model simulates Cl abundances relatively well, with values that are from 25% low to slightly high compared to observations in the lower stratosphere [*Flocke et al.*, 1999], depending on latitude and season. Similarly, modeled OH radical abundances are about 20% lower than observations in the lower stratosphere [e.g., *Hanisco et al.*, 2001]. Although no $O(^1D)$ observations exist to test model predictions, photolysis rate coefficients for O_3 and the quantum yields to produce $O(^1D)$ are well known. To zeroth order, then, we estimate the error in predicted $O(^1D)$ to be dominated by the error in predicted O_3. The LLNL 2-D model predicts ozone mixing ratios that are within −10% and +20% of observations at 20 km (depending on latitude and season) and within ±10% at 30 km [see *Park et al.*, 1999]. Thus, errors in $O(^1D)$ are not predicted to be large. The sensitivities of modeled isotopic compositions to these known biases are estimated in section 4.4. Additional chemical processes that have recently come to our attention but which have not been included in these runs of the LLNL 2-D model include a 15% faster rate for quenching of $O(^1D)$ by N_2 [*Ravishankara et al.*, 2002], the suggested increase in the rate for CH_4 + Cl [*Michelsen*, 2001], and a faster production rate of OH from HNO_4 photolysis [*Roehl et al.*, 2002].

3.2. Model Transport and Isotopic Compositions

[22] In addition to sensitivities to absolute rates of chemical reactions and mixing ratios of radicals, it is well known a priori that isotopic compositions will also depend on stratospheric transport and mixing. Both transport and mixing act to reduce the average isotopic fractionation observed relative to that which would occur in a strictly isolated air mass. This concept is discussed at length in Part 1. For completeness, a short description is given here.

[23] The Rayleigh distillation equation (equation (1)) describes the change in the isotopic composition of CH_4 after a given amount of CH_4 has been destroyed (i.e., for a given ratio of $[CH_4]/[CH_4]_0$, with $[CH_4]_0$ defined as the mixing ratio for air entering the stratosphere):

$$\ln\left(\frac{[CH_4]}{[CH_4]_0}\right) = \left(\frac{\alpha}{1-\alpha}\right) * \ln\left(\frac{[1000+\delta^{13}C]}{[1000+\delta^{13}C_0]}\right). \quad (1)$$

In an isolated, well-mixed system, $\alpha = \alpha^c_{KIE}$ where α^c_{KIE} is the oxidant-weighted isotope fractionation factor given by

$$\alpha^C_{KIE} = \frac{k_{OH}}{k^{13}_{OH}} f_{OH} + \frac{k_{Cl}}{k^{13}_{Cl}} f_{Cl} + \frac{k_{O(1D)}}{k^{13}_{O(1D)}} f_{O(1D)} \quad (2)$$

and f_x is the fraction of CH_4 oxidized by OH, Cl, or $O(^1D)$. A similar expression is used for hydrogen isotope fractionation where δD, α^D_{KIE}, and relative rates for the reactions of OH, Cl, and $O(^1D)$ with CH_4 versus those for CH_3D (i.e., the hydrogen KIEs) are substituted for $\delta^{13}C$, α^c_{KIE}, and the carbon KIEs for reaction of the oxidants with CH_4 and $^{13}CH_4$ in equations (1) and (2). Note that f_{OH}, f_{Cl}, and $f_{O(1D)}$ are the same whether carbon or hydrogen fractionation is considered.

[24] In a system such as the stratosphere, which is not isolated nor well-mixed with respect to CH_4, the apparent fractionation factor, α_{app}, derived from observations when the observations are plotted in the form of equation (1), will always be smaller than that given by the "chemistry only" α_{KIE} defined in equation (2). While this attenuation of α_{KIE} by transport can be shown mathematically, it can easily be explained conceptually. Suppose, for example, that two air parcels with different amounts of CH_4 are mixed together. Even if the isotopic compositions of the CH_4 in each individual air parcel had previously obeyed simple Rayleigh isotope fractionation with a fractionation factor α_{KIE}, the act of mixing these two air parcels together necessarily means that Rayleigh fractionation no longer describes the isotope: CH_4 relationship in the resulting mixture. The mixing of air masses attenuates the isotope fractionation expected from the pure Rayleigh relationship because mixing of an air parcel that has more CH_4 (and therefore a lighter isotopic composition) with an air parcel that has less CH_4 (and therefore a heavier isotopic composition) reduces (i.e., "lightens") the isotopic composition at the resulting CH_4 mixing ratio of the mixture from that which would be predicted simply by the underlying kinetic isotope effect (i.e., by the Rayleigh equation with $\alpha = \alpha_{KIE}$). While it is still possible, though not necessary, that a Rayleigh-type relationship could be used to describe the isotope:tracer relationship in the resulting mixtures of air parcels, the apparent fractionation factor α_{app} is necessarily less than α_{KIE}.

[25] For application to the stratosphere, note that this reduction in α_{app} from α_{KIE} is true regardless of the type of mixing occurring - that is, whether the nature of the mixing or transport is similar to end-member mixing between polar vortex and midlatitude air [e.g., *Waugh et al.*, 1997; *Michelsen et al.*, 1998; *Herman et al.*, 1998; *Rex et al.*, 1999], continuous weak isentropic mixing across the polar vortex edge during the time of maximum descent [e.g., *Plumb et al.*, 2000], the constant input of CH_4 from the troposphere, or simply the finite transport and mixing times between regions of the stratosphere which have different chemical lifetimes for CH_4 (see Part 1 for further discussion). In general, the combination of all mixing processes reduces the average isotopic fractionation factor α_{app} below that predicted by α_{KIE}. The degree to which model transport simulates transport occurring in the stratosphere must therefore also be considered.

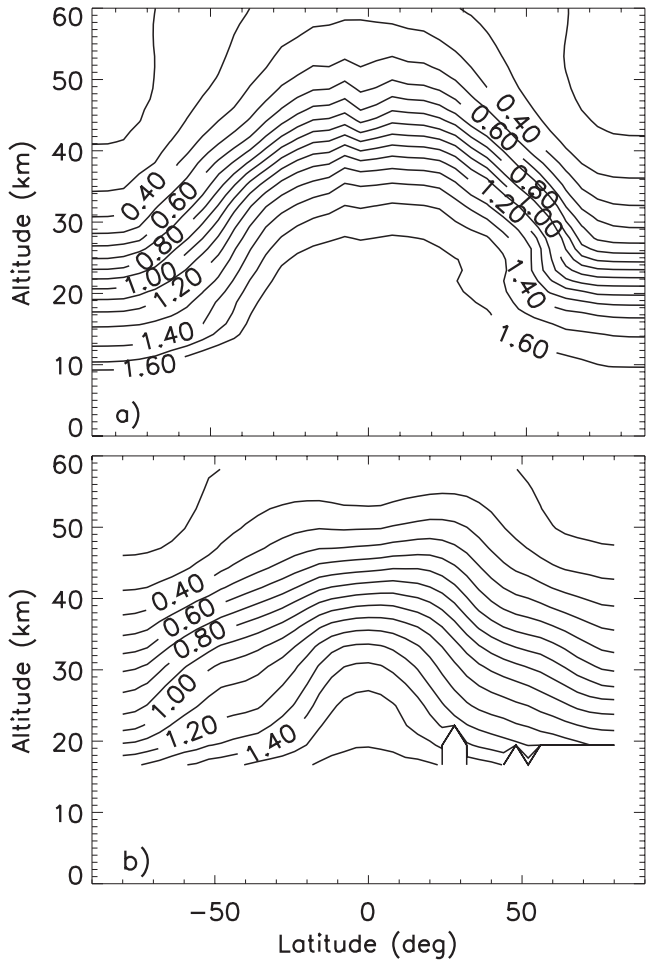

Figure 2. (a) Annual mean CH_4 mixing ratios simulated by the LLNL 2-D model as a function of pressure altitude and latitude. (b) Annual mean CH_4 mixing ratios from the CLAES and HALOE instruments aboard the Upper Atmosphere Research Satellite as a function of pressure altitude and latitude [*Randel et al.*, 1998]. Contour intervals for CH_4 are 0.2 ppmv.

[26] Comparisons of LLNL 2-D model results with observations of CH_4 mixing ratios, stratospheric mean ages, and with results from other 2-D and 3-D models have been made [e.g., *Park et al.*, 1999; *Hall et al.*, 1999]. Modeled CH_4 mixing ratios as a function of latitude and pressure altitude are shown in Figure 2a, while CLAES and HALOE satellite observations [*Randel et al.*, 1998] are shown for comparison in Figure 2b. As expected, the model results capture the characteristic pattern of CH_4 oxidation increasing in general as a function of altitude, superimposed on the stratospheric circulation (upwelling in the tropics and downwelling in the extratropics). However, we note that air characteristic of the tropics clearly extends too far into the extratropics in the model, up to 50°N and S. This feature is also reflected in comparisons of modeled CH_4:N_2O correlations with Atmospheric Trace MOlecule Spectroscopy (ATMOS) measurements from the Space Shuttle [*Michelsen et al.*, 1998] (Figure 3); the modeled CH_4:N_2O correlations also exhibit a tropical character for all model latitudes equatorwards of 50°. Importantly,

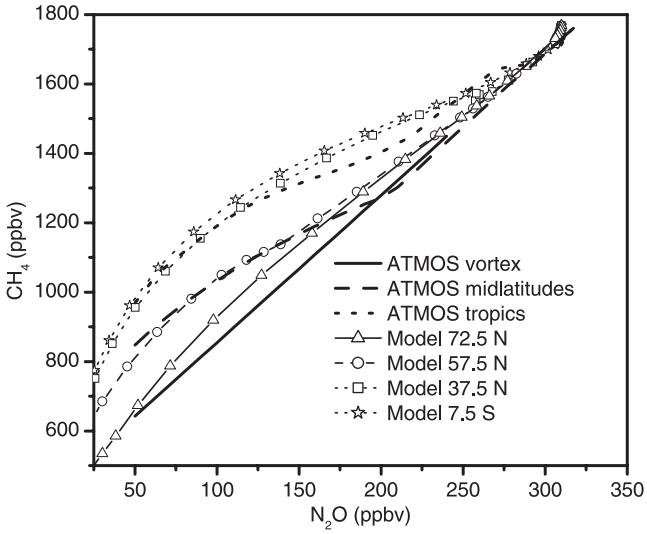

Figure 3. CH_4:N_2O correlations at different latitudes from ATMOS observations (lines) and the LLNL model (symbols). ATMOS observations are from 1992 to 1994 [*Michelsen et al.*, 1998], while the model simulates CH_4 mixing ratios more appropriate for 1997–2000, so the ATMOS relationships shown here have been offset by 50 ppbv. The modeled CH_4:N_2O correlation at 37.5°N exhibits a characteristically tropical relationship, while that at 57.5°N has a shape more characteristic of midlatitude air.

however, the model simulates the differences between the tropical, midlatitude, and high latitude CH_4:N_2O correlations quite well, if we discount where the model's midlatitudes begin. Because our isotope analysis here also involves comparing the correlations between modeled and observed long-lived tracers (since δ^{13}C-CH_4, δD-CH_4, and CH_4 can all be considered long-lived tracers), the ability of the LLNL 2-D model to simulate the differences between the tropical, midlatitude, and high latitude correlations for the two long-lived tracers CH_4 and N_2O is the feature of the model most relevant for this study. Lastly, we note that comparisons of SF_6 and CO_2 mean-age tracers with LLNL 2-D model results have also been made and show that the LLNL model mean ages are too small relative to observations throughout the stratosphere by a factor of 2 [*Park et al.*, 1999; *Hall et al.*, 1999]. This discrepancy is a common problem for virtually all 2-D and 3-D models, and a self-consistent solution to the problem(s) is an active area of research [e.g., *Hall et al.*, 1999; *Eluszkiewicz et al.*, 2000]. Although it is not yet clear why the transport formulations of 2-D models yield mean ages which are too low, it may in part indicate that diffusive transport in the models is too weak. The possible effects of weak diffusive transport on modeled isotopic compositions will be discussed in detail in section 4.4.

[27] In summary, a complete analysis of discrepancies between model results and observations should consider all the possible sensitivities to chemical rates, radical abundances, and transport. Despite the range of possible errors, we find in the analysis below that chemistry and transport are modeled sufficiently well to understand the basic factors controlling the isotopic compositions of CH_4 in the stratosphere. This conclusion is based on (1) comparisons of model results with ER-2 isotope observations and ATMOS CH_4:N_2O observations, (2) estimates of errors in predicted isotopic compositions resulting from known chemistry biases in the LLNL 2-D model, (3) the sensitivity studies of *Wang et al.* [2002] noted above, and (4) the double constraint on the integrated histories of oxidation and transport by the δ^{13}C-CH_4 and δD-CH_4 measurements on the same ER-2 samples. Furthermore, we can test the sensitivity of the modeled isotopic compositions to different values of experimental KIEs, but only to within the uncertainties of model error in chemistry and transport (see sections 4.4 and 4.5).

4. Results and Discussion

[28] In the following sections, we compare 2-D model results with new observations of δ^{13}C-CH_4 and δD-CH_4 from the ER-2 aircraft [*Rice et al.*, 2003] with the goals of determining how well the 2-D model reproduces the observations and what factors are responsible for the observed increase in the apparent isotopic fractionation factors with decreasing methane mixing ratios in the ER-2 samples (sections 4.1 to 4.3). We then estimate the effects of known biases in model chemistry and transport on predicted isotopic compositions in section 4.4. In section 4.5, we examine the sensitivity of the predicted isotopic compositions to different values for the KIEs using the scenarios in Tables 3 and 4 and evaluate whether these sensitivities are large enough to differentiate from possible modeling errors. Finally, in section 4.6 we briefly outline how the isotopic compositions of CH_4 may be used as a diagnostic of integrated chemistry and transport in model-model intercomparisons.

4.1. Model Results for δ^{13}C-CH_4 and Comparison With Observations

[29] Model results for annual mean δ^{13}C-CH_4 using the carbon KIEs of Scenario C_S1 from Table 1 are shown in Figure 4 as a function of latitude and pressure altitude. As CH_4 is oxidized, the remaining CH_4 becomes enriched in ^{13}C (e.g., compare Figure 4 with Figure 2a). Enrichment is expected based on the carbon KIEs for the CH_4 sink reactions with OH, Cl, and O(^{1}D). The KIEs are all greater than 1, hence δ^{13}C-CH_4 will increase regardless of where CH_4 is oxidized in the stratosphere. However, the value of the instantaneous oxidant-weighted carbon KIEs (i.e., α_{KIE} in equation (2)) depends on latitude and altitude primarily because the absolute and relative abundances of OH, Cl, and O(^{1}D) depend on latitude and altitude. For example, model predictions for the instantaneous fractions of CH_4 oxidized by OH, Cl, and O(^{1}D) (i.e., the values for f_{OH}, f_{Cl}, and $f_{O(1D)}$) averaged over one year are shown in Figure 5. The fractionation factors for these three oxidants combine to yield the annually averaged α_{KIE} for Scenario C_S1 shown in Figure 6.

[30] Enrichment in ^{13}C as CH_4 mixing ratios decrease is also expected based on previous δ^{13}C-CH_4 observations [*Wahlen et al.*, 1989; *Brenninkmeijer et al.*, 1995; *Sugawara et al.*, 1997]. The new ER-2 data, however, extend to lower CH_4 mixing ratios than any previous observations, are almost an order of magnitude more numerous than the other

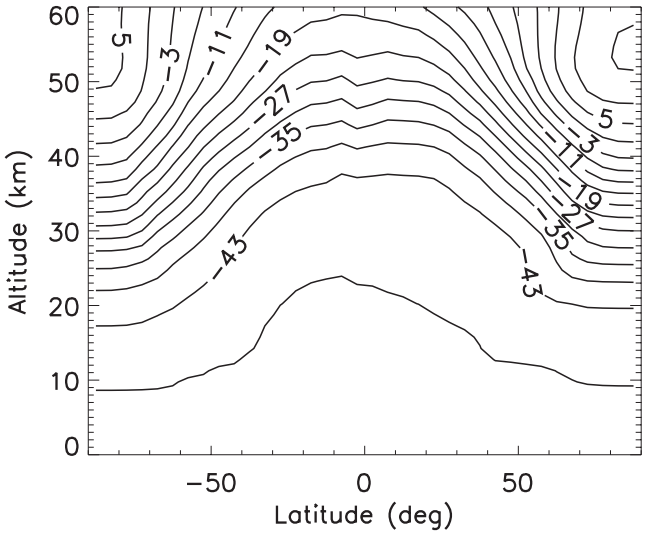

Figure 4. Annual mean δ^{13}C-CH_4 (in ‰ versus V-PDB) simulated by the LLNL 2-D model using the set of KIEs from model scenario C_S1 as a function of pressure altitude and latitude.

studies, and cover a broad range of latitudes (1°S–89°N), altitudes (8.6–20.8 km), seasons (northern winter, spring, and summer), and years (1996, 1997, and 2000) [*Rice et al.*, 2003]. Moreover, the low CH_4 mixing ratio observations are from air collected in the polar vortex (or in polar vortex remnants) which has descended to ER-2 altitudes via the stratospheric circulation; these vortex samples therefore represent isotope fractionation occurring far above the ER-2 ceiling.

[31] Because latitude and altitude are not conserved variables in the stratosphere, it is best to plot values for δ^{13}C-CH_4 against CH_4 mixing ratios (Figure 7) (For a discussion of tracer:tracer correlations in general, see, e.g., *Plumb and Ko* [1992] and *Waugh et al.* [1997]). In addition, such a plot is particularly valuable for comparing the highly spatially resolved aircraft observations with global-scale model results. The shaded region in Figure 7 represents the envelope of the modeled δ^{13}C:CH_4 relationships for Scenario C_S1 throughout the stratosphere for all 12 model months. The modeled δ^{13}C:CH_4 relationships for the month of March in the tropics (at 7.5°S) and in the extratropics (72.5°N) for Scenario C_S1 are indicated by the small triangles and the bold solid line, respectively. Interestingly, the difference in the predicted δ^{13}C:CH_4 relationships between the tropics and the extratropics is primarily due to transport. As discussed in section 3.2, the mixing of air masses always results in a reduction of the isotopic fractionation relative to that which would result in a strictly isolated air mass. Since the tropics are relatively isolated and less influenced by transport and mixing compared with the extratropics, tropical δ^{13}C-CH_4 values are heavier (i.e., more fractionated) for a given CH_4 mixing ratio than in the extratropics. Thus, model transport attenuates the apparent fractionation factors, α_{app}, in the extratropics more than in the tropics, as expected, and more than compensates for the smaller tropical α_{KIE}'s (see Figure 6). The tropical ER-2 δ^{13}C-CH_4 observations are also on average heavier for a given CH_4 mixing ratio than those from the extratropics [see *Rice et al.*, 2003]. The minimum CH_4 mixing ratio for samples collected by the ER-2 in the tropics, however, is 1604 ppbv. Thus, tropical δ^{13}C-CH_4 measurements to test the model predictions at lower CH_4 mixing ratios will require samples collected by high-altitude balloon.

[32] To judge how well the LLNL 2-D model predicts the δ^{13}C:CH_4 relationship in the extratropics, we compare the ER-2 observations with model predictions for March at 72.5°N in Figure 7. The month and latitude were chosen because most ER-2 samples with CH_4 mixing ratios less than 1300 ppbv were collected in March or April in the Arctic vortex or in remnants of the vortex at high latitudes [*Rice et al.*, 2003]. This choice does not significantly affect our assessment of the model results, however, for the following reasons: (1) model predictions from the high latitudes in general (e.g., 67.5 to 90°N) yield results that are essentially identical to those shown for 72.5°N, (2) no enhancement in δ^{13}C-CH_4 due to reaction with elevated Cl

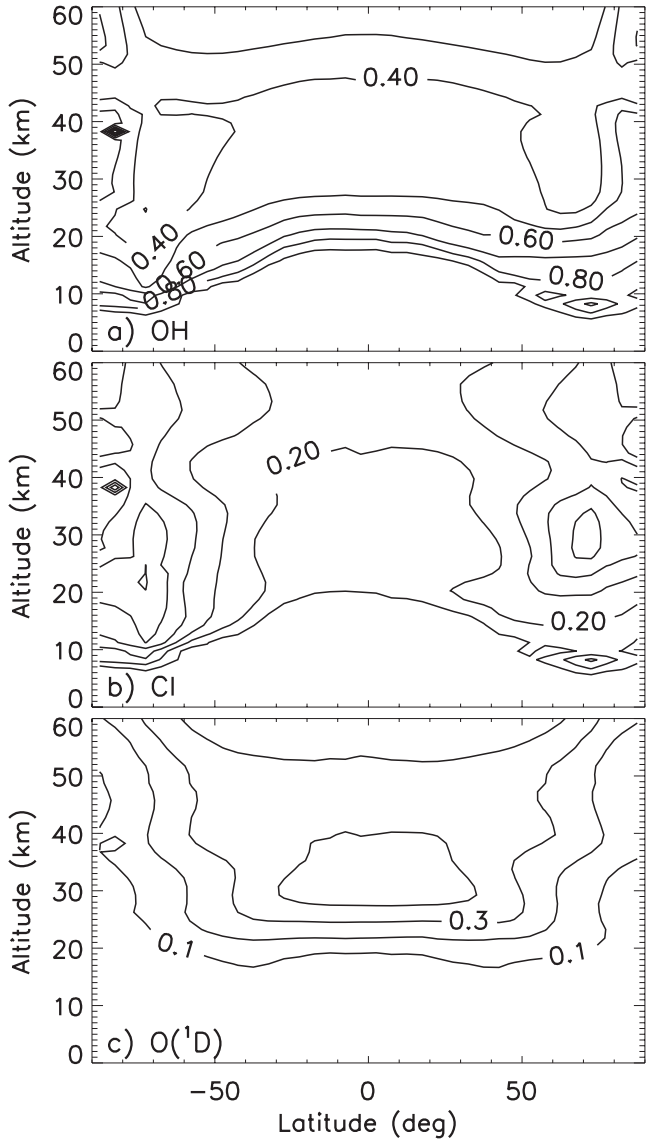

Figure 5. Annual average values for (a) f_{OH}, (b) f_{Cl}, and (c) $f_{O(1D)}$ as a function of latitude and pressure altitude.

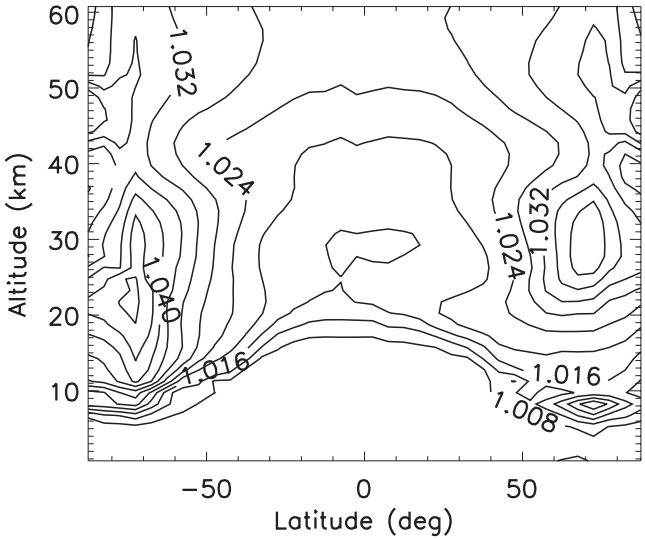

Figure 6. Annual average of the instantaneous carbon KIEs weighted by the oxidant loss rates (α^{C}_{KIE}) as a function of latitude and pressure altitude for scenario C_S1.

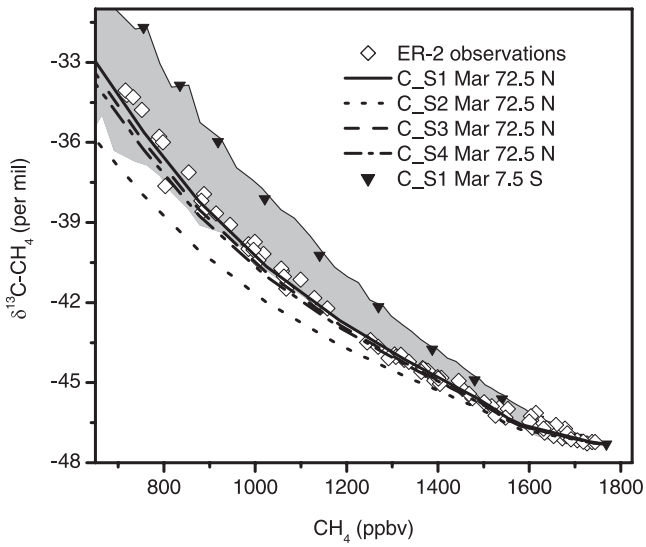

Figure 7. The correlation between δ^{13}C-CH_4 and CH_4 for ER-2 measurements and model scenarios. The shaded region represents the envelope of model results from Scenario C_S1 for δ^{13}C:CH_4 for all model latitudes and months. Model results for scenarios at 72.5°N are indicated by lines, while results at 7.5°S are indicated by triangles. The ER-2 observations are plotted as diamonds.

in the lower stratosphere winter polar vortices was detected in either the model results nor the observations [see *Rice et al.*, 2003], and (3) predicted δ^{13}C:CH_4 relationships are not particularly sensitive functions of latitude or season at high CH_4 mixing ratios.

[33] Using Figure 7, we can evaluate the LLNL model scenarios incorporating different sets of carbon KIEs through comparison with ER-2 observations. For CH_4 mixing ratios greater than 1200 ppbv, all model scenarios predict the observed extratropical δ^{13}C:CH_4 relationship to better than ±0.5‰, except for Scenario C_S2, the one scenario that includes the small O(^{1}D) KIE of 1.001. In contrast, for CH_4 mixing ratios less than 1200 ppbv, all scenarios predict δ^{13}C-CH_4 values that are lighter for a given CH_4 mixing ratio than the observations. Scenario C_S1 yields the steepest (i.e., isotopically "heaviest") δ^{13}C:CH_4 relationship but one which is still lighter than the ER-2 observations by ~0.5‰ for CH_4 < 800 ppbv. Results from Scenarios C_S3 and C_S4 are lighter than those of C_S1, as expected for the smaller OH and Cl KIEs. However, these differences are small (<1‰) even at low mixing ratios of CH_4. Thus, it does not appear that the differences between the KIEs used in scenarios C_S1, C_S3, and C_S4 are large enough to be distinguished from possible errors in chemistry and transport. This point will be discussed further in section 4.4. In contrast, results from Scenario C_S2 are much lighter than the other 3 scenarios, deviating by 1 to 3.5‰ from the observations between 1200 to 716 ppbv, respectively. Thus, using the smaller O(^{1}D) KIE of 1.001 results in a relatively large difference between the model predictions and the observations in both the magnitude and curvature of the δ^{13}C:CH_4 relationship.

[34] A comparison of 2-D model results with measurements of δ^{13}C-CH_4 and CH_4 in air collected in August 1994 at midlatitudes over Japan (38.3 to 40.0°N) between 14.0 and 34.7 km by a balloon-borne cryogenic sampler [*Sugawara et al.*, 1997] can also be made. The balloon observations are compared with model results for August at 37.5°N and 57.5°N in Figure 8. If a straight comparison of model results at 37.5°N with the midlatitude observations is made, it would appear that Scenario C_S2, with the smaller O(^{1}D) KIE, best reproduces the observations, which is the opposite of what was found for the ER-2 observations. However, as discussed in section 3.2 and shown in Figure 3, the tracer: tracer correlations produced by the LLNL model only begin to have midlatitude character polewards of 50°N while the correlations at model latitudes <50°N are more characteristic of the tropics. Since modeled values of δ^{13}C-

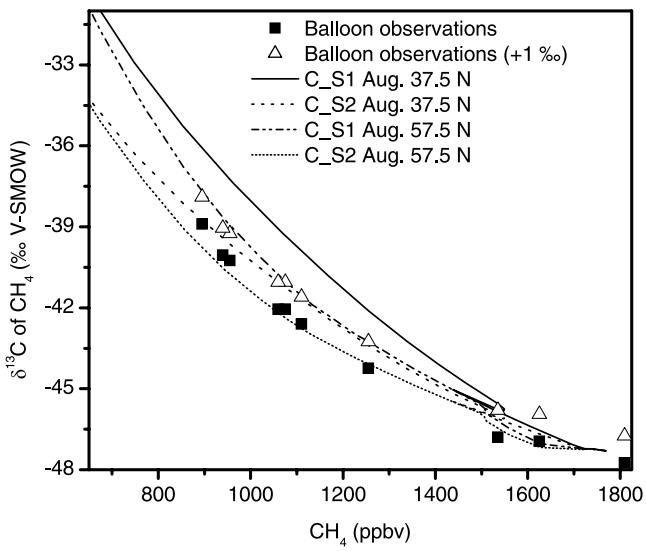

Figure 8. The correlation between δ^{13}C-CH_4 and CH_4 from model results (lines) and from balloon observations [*Sugawara et al.*, 1997] (squares).

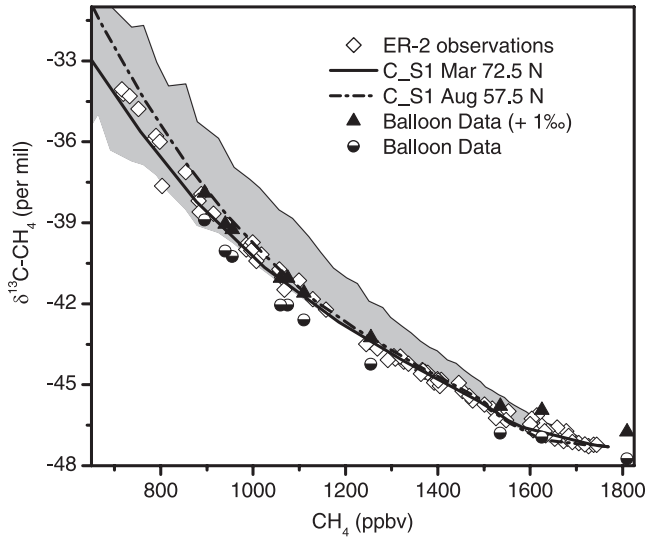

Figure 9. The correlation between δ^{13}C-CH_4 and CH_4 from model results (lines), ER-2 observations (diamonds), and the balloon observations from *Sugawara et al.* [1997] which have been arbitrarily shifted by +1‰ (triangles). The original balloon observations are shown as the half-filled circles. The shaded region represents the envelope of model results from Scenario C_S1 for δ^{13}C:CH_4 for all model latitudes and months.

CH_4 for Scenario C_S1 at 57.5°N are significantly lighter than those at 37.5°N, as expected for the transition from tropical to extratropical air, a comparison of model results from 57.5°N with the balloon observations reduces the model-measurement discrepancy to about +1‰ for Scenario C_S1. Moreover, the curvature of the δ^{13}C:CH_4 relationship between 800 and 1300 ppbv CH_4 produced by Scenario C_S1 more closely resembles the balloon observations than C_S2. To quantitatively assess this, we fit the model results and the balloon and ER-2 observations with logarithmic functions of the form $\delta^{13}C = m * \ln(CH_4) + \delta^{13}C_0$, where m is a measure of the "curvature." The value of m for C_S2 at both 57.5 and 37.5°N is more than a factor of two farther from the Sugawara observations than that for C_S1. The C_S1 curvature term is also closer to the ER-2 observations. Intuitively, this curvature indicates the increasing importance of the large $O(^1D)$ KIE in older air for capturing the shape of the δ^{13}C:CH_4 relationship. Thus, Scenario C_S1 best captures both the δ^{13}C:CH_4 correlation and its curvature from the ER-2 observations and the δ^{13}C:CH_4 curvature from the balloon observations. However, a 1‰ discrepancy still remains between the model results for C_S1 and the balloon observations and between the ER-2 and the balloon observations.

[35] In Figure 9, ER-2 observations are plotted with the balloon observations, the balloon observations offset by +1‰, and model results. The agreement between the offset balloon and the ER-2 observations is quite good for CH_4 < 1600 ppbv, with scenario C_S1 reproducing both sets of observations to within 0.5‰ or better. Possible explanations for the difference of 1‰ between the ER-2 and balloon observations are discussed in detail in *Rice et al.* [2003]. For this analysis, if we arbitrarily assume that there is a systematic offset of ~1‰ between the balloon and the ER-2 δ^{13}C-CH_4 measurements, then there is little difference between the balloon and the ER-2 δ^{13}C:CH_4 relationships for CH_4 < 1600 ppbv which is not captured by Scenario C_S1. Determining the source of the discrepancy between the ER-2 and balloon observations, if real, will require additional balloon stratospheric measurements and/or an intercomparison of laboratory standards for resolution. At present, however, there appears to be no other reasonable way to resolve the model-measurement-measurement discrepancy. Indeed, *Wang et al.* [2002] came to the same conclusion that the $O(^1D)$ KIE of 1.013 gave a more realistic δ^{13}C:CH_4 relationship based on the balloon observations alone using a 2-D model with very different chemistry and transport (see, e.g., *Park et al.* [1999] for a comparison of LLNL 2-D model and Harvard 2-D model transport and chemistry simulations). In section 4.4, we will examine in detail the possible effects that model errors in transport and chemistry may have on this conclusion, after discussion of the additional constraint from the simultaneous observations of δD-CH_4.

[36] Despite some uncertainties at the level of ~1‰, the LLNL 2-D model certainly captures to first order the combined effects of chemistry and transport on the δ^{13}C:CH_4 relationships. Therefore, the model can be used to refine the analysis in Part 1 that used a 0-D, chemistry-only Rayleigh fractionation model [*Rice et al.*, 2003]. Isotope geochemists analyzing isotope fractionation in a variety of environmental settings also plot isotopic compositions versus mixing ratios, although usually in the form of equation (1). The slope of the line when the data are plotted in logarithmic form (or an exponential fit to the data as plotted in Figure 7) yields the apparent isotope fractionation factor, α_{app}. For the ER-2 observations, α_{app} increases as CH_4 mixing ratios decrease [*Rice et al.*, 2003]. The empirically derived values for α_{app} ranged from 1.0105 ± 0.0004 at the highest observed stratospheric CH_4 mixing ratio to 1.0204 ± 0.0004 at the lowest observed CH_4 mixing ratio, while a fit to all the observations (between 716 and 1720 ppbv) yielded 1.0154 ± 0.0008. For comparison, a Rayleigh-type fit to the Scenario C_S1 results in Figure 7 from 650 to 1700 ppbv CH_4 yields an overall average α_{app} range of 1.0155 ± 0.0004 and a similar trend of increasing values for α_{app} with decreasing CH_4. This agreement is expected based on the close agreement of the model results and the observations. In Part 1, changes in f_{OH}, f_{Cl}, and $f_{O(1D)}$ were empirically deduced as the likely explanation for these changes in α_{app} as a function of CH_4 mixing ratio. This interpretation is confirmed by the agreement of the model results and observations and an examination of the corresponding modeled values for f_{Cl}, f_{OH}, and $f_{O(1D)}$ in Figure 5. The fractionation factor increases as f_{Cl} and $f_{O(1D)}$ increase with altitude and mean age due to increased Cl and $O(^1D)$ radical mixing ratios, as seen in Figure 6. Due to the small temperature dependence of the Cl KIE, stratospheric temperature differences have a negligible impact on the curvature of the modeled δ^{13}C:CH_4 relationship.

4.2. Model Results for δD-CH_4 and Comparison With Observations

[37] Only two previous studies have reported measurements of δD-CH_4 in the stratosphere [*Wahlen et al.*, 1989;

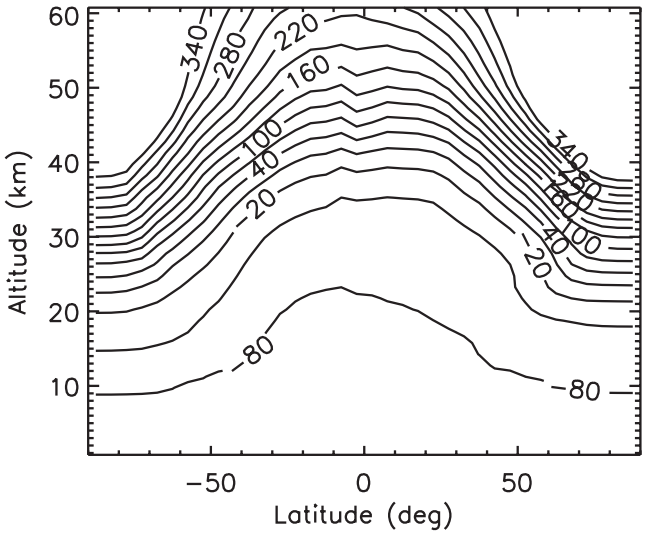

Figure 10. Annual mean δD-CH_4 (in ‰ versus V-SMOW) simulated by the LLNL 2-D model using the set of KIEs from model scenario D_S1 as a function of pressure altitude and latitude.

Irion et al., 1996]. Due to the relatively few measurements of the unpublished data set of Wahlen et al. and the low precision of the remote sensing observations of Irion et al., the high-precision ER-2 δD-CH_4 observations reported in Part 1 provide new and much stronger constraints for modeling isotope fractionation in the stratosphere. Model results for δD-CH_4 as a function of pressure altitude and latitude are shown in Figure 10 using the hydrogen KIEs in Scenario D_S1. The difference between modeled tropospheric and stratospheric δD-CH_4 values are large, ranging from −90‰ in the troposphere to greater than +200‰ at high latitudes in the upper stratosphere. Annually averaged instantaneous hydrogen KIEs weighted by the oxidant loss rates (α_{KIEs}) are shown in Figures 11a and 11b for scenarios D_S1 and D_S5, respectively.

[38] In order to compare the model results with the ER-2 observations, δD-CH_4 is plotted against CH_4 mixing ratio in Figure 12. As for δ^{13}C-CH_4, model results from 72.5° N in March were chosen because most ER-2 samples with CH_4 mixing ratios less than 1300 ppbv were collected in March or April in the Arctic vortex or in remnants of the vortex at high latitudes. Similar to Figures 6 and 8 for δ^{13}C:CH_4, the shaded regions in Figure 12 represent the envelope of all modeled δD:CH_4 relationships throughout the stratosphere for (a) Scenario D_S1 and (b) Scenario D_S5. For CH_4 mixing ratios <1200 ppbv, Scenarios D_S1, D_S3, and D_S4 predict δD-CH_4 values that are heavier than the ER-2 measurements. Results for Scenario D_S1 are heavy by ∼10 to 15‰ depending on CH_4 mixing ratio. Scenarios D_S3 and D_S4 are variants of Scenario DS_1 in which the activation energies for the experimental KIEs for CH_4 + OH and CH_4 + Cl are lowered by their 1σ and 2σ experimental precisions, respectively. Lowering either KIE still results in δD-CH_4 results that are heavy by ∼5−10‰ compared with the observations. Note that using the *Tyler et al.* [2000] Cl KIE of 0.894exp(145/T), which has a larger KIE at stratospheric temperatures (see Figure 1c), would yield results even heavier than those for D_S1. Scenario D_S5 using the OH KIE from *DeMore* [1993] yields model results that are within ±5‰ of the observations for CH_4 < 1200 ppbv. Scenario D_S2, which assumes an O(^{1}D) KIE of unity, results in δD-CH_4 values that are ∼5 ‰ lighter than the observations for CH_4 < 1100 ppbv. Between CH_4 mixing ratios of ∼1200 and 1650 ppbv, all model scenarios predict δD-CH_4 values that are heavier than the observations by up to 10‰ despite the fact that the model is prescribed to match the δD:CH_4 relationship for air entering the stratosphere (i.e., at 1720 ppbv CH_4). Interestingly, this latter result is in direct contrast to the best model results for the δ^{13}C:CH_4 relationship that closely matched the observations over this range of CH_4. Since CH_4 oxidation in the lower stratosphere is dominated by OH (e.g., Figure 5), it is possible that the model-observation discrepancy may be due to the hydrogen OH KIEs used or model radical abundances. Alternatively, model transport could be too weak in the lower stratosphere and thus might not adequately attenuate the α_{KIE} to reproduce the observed α_{app}. Distinguishing between these possibilities will be discussed further in sections 4.4 and 4.5 in the context of the additional constraint from the δ^{13}C-CH_4 observations.

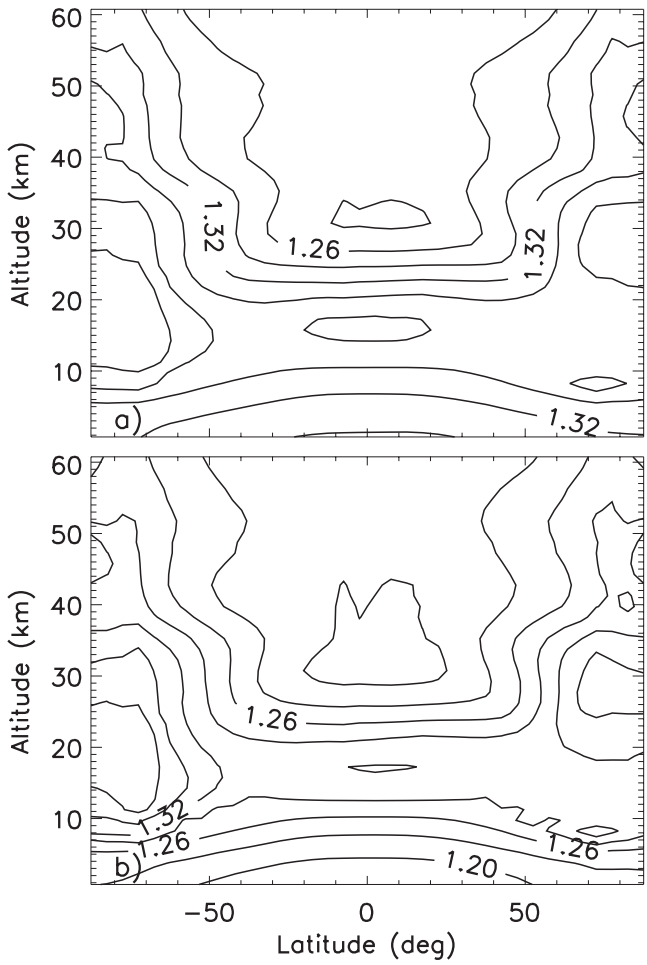

Figure 11. Annual average of the instantaneous hydrogen KIEs weighted by the oxidant loss rates (α^{H}_{KIE}) as a function of latitude and pressure altitude for (a) Scenario D_S1 and (b) Scenario D_S5.

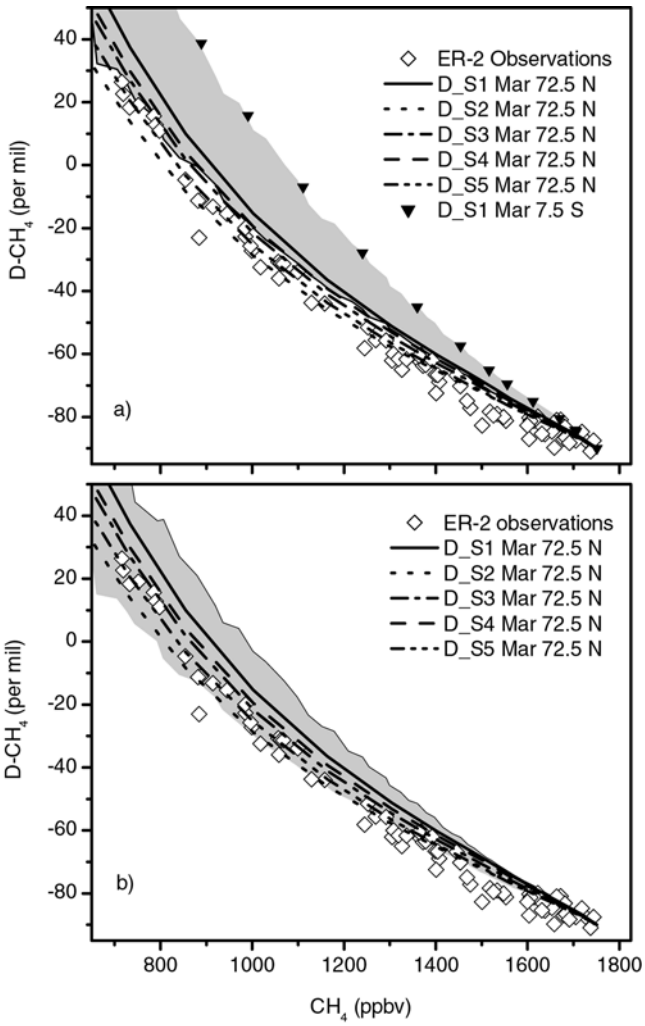

Figure 12. The correlation between δD-CH_4 and CH_4. The shaded regions represent the envelope of model results for (a) Scenario D_S1 and (b) Scenario D_S5 for all model latitudes and months. Model results for scenarios at 72.5°N are indicated by lines, while results at 7.5°S are indicated by triangles. The ER-2 observations are plotted as diamonds.

[39] Rayleigh-derived average fractionation factors, α_{app}, obtained from the slope of the δD:CH_4 relationship of the ER-2 measurements increase monotonically from 1.115 ± 0.008(2σ) to 1.198 ± 0.008(2σ) from high to low CH_4 mixing ratio ranges, respectively [*Rice et al.*, 2003]. If a single exponential is used to fit all the stratospheric data, Rice et al. obtained a value of 1.153 ± 0.010(2σ). For comparison, a Rayleigh-type fit to the Scenario D_S5 results in Figure 12b from 650 to 1700 ppbv CH_4 yields an overall average α_{app} range of 1.153 ± 0.004 and an increasing α_{app} with decreasing CH_4 mixing ratio. The primary driver of the increasing α_{app} for hydrogen fractionation is the increasing influence of Cl with mean age. In contrast to the α_{app} for δ^{13}C-CH_4, the increase in $f_{O(1D)}$ for hydrogen will reduce the α_{app} since the $O(^1D)$ KIE is the smallest of the three. To test whether the temperature dependence of the KIEs plays a role in the increase in α_{app}, a model run with all KIEs set to their values at 225 K yielded no significant change in the curvature of the δD:CH_4 relationship. Thus, we conclude that the change in α_{app} is primarily due to the change in f_{Cl} and not temperature.

4.3. Comparing the Modeled and Measured δD-CH_4:δ^{13}C-CH_4 Relationship

[40] A scatterplot of δD-CH_4 versus δ^{13}C-CH_4 for the ER-2 observations is compared with model results for various KIE scenarios in Figure 13. Both observations and model results show a remarkably linear relationship. As noted in *Rice et al.* [2003], a compact correlation between δD-CH_4 and δ^{13}C-CH_4 is expected. Both isotopologues are long-lived with respect to vertical and horizontal transport timescales, which is the only requirement for a linear correlation in the stratosphere [e.g., *Plumb and Ko*, 1992], and they are obviously further correlated chemically as well. The slope of the observed linear correlation is 8.6 ± 0.8. The two sets of carbon and hydrogen KIE scenarios which come closest to reproducing the observations are the combination of D_S5 with C_S1, with a slope of 9.0, and of D_S2 with C_S1, with a slope of 8.3. That these particular scenario combinations have slopes which are closest to the observations is simply due to the fact that they produce the steepest δ^{13}C:CH_4 relationship (C_S1) and the flattest δD:CH_4 relationships (D_S5 and D_S2). Thus, the slope gives a relative measure of the effects of integrated CH_4 oxidation and transport on the carbon and hydrogen isotopic compositions in the stratosphere and may therefore be an efficient means of comparing these effects in models using the same set of KIEs. It is also important to note that the slope of the modeled δD:δ^{13}C relationship is relatively insensitive to the latitude or season chosen (Figure 13). This insensitivity is in direct contrast to the isotope:CH_4 relationships explored in sections 4.1 and 4.2, which are significantly different in the tropics, midlatitudes, and high latitudes. However, varying the KIEs and, by proxy, chemistry, does result in large changes in the δD-δ^{13}C slope. Since all model runs used identical chemistry and transport, differences in slopes for the different combinations of scenarios in Figure 13 result only from differences in the

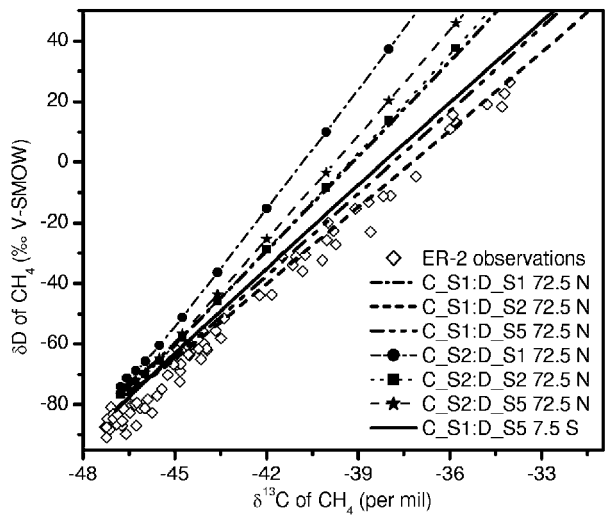

Figure 13. δD-CH_4 versus δ^{13}C-CH_4 for the ER-2 observations (diamonds) and model results (lines). Model points from the troposphere are not plotted.

KIEs used. Thus, the slope of the δD:$\delta^{13}C$ relationship may be a useful and efficient method of testing integrated model chemistry and transport in model-model intercomparisons with a given set of KIEs (see section 4.6).

4.4. Estimates of the Effects of Model Errors in Chemistry and Transport on Isotopic Compositions

[41] Discrepancies between the model results and observations may be caused by errors in model chemistry, model transport, laboratory KIEs, measurement errors, or some combination of these factors. In this section, we estimate the possible effects of model chemistry and transport errors on predicted isotopic compositions. In order to simplify the discussion, we assume that possible measurement errors for the ER-2 data are negligible by comparison. We first use the known or estimated errors in the modeled OH, Cl, and $O(^1D)$ abundances to determine if changes in each individual oxidant would improve or reduce the agreement between model results and observations for both $\delta^{13}C$-CH_4 and δD-CH_4. Since the modeled $\delta^{13}C$:CH_4 relationship is too light for all scenarios while the modeled δD:CH_4 relationship is generally too heavy, any change made to modeled radical abundances that would improve the model:measurement agreement must simultaneously alter the two predicted isotopic compositions in opposite directions. Thus, the combination of $\delta^{13}C$-CH_4 and δD-CH_4 ER-2 observations provides a constraint on whether chemistry errors alone can account for the model-observation discrepancies. Similarly, we examine possible transport errors and discuss whether changes in model transport alone would improve or degrade the model-measurement agreement for both $\delta^{13}C$-CH_4 and δD-CH_4.

[42] Upper limits for the change in predicted isotopic compositions caused by altering model radical abundances can be estimated through Rayleigh calculations using equations (1) and (2). Since the calculations are made assuming that (1) the largest changes in the values for α^{C}_{KIE} and α^{H}_{KIE} anywhere in the stratosphere resulting from a particular change in radical abundance(s) are valid everywhere in the stratosphere and (2) there is no attenuation of the α_{KIE}'s by transport, these estimates should grossly overpredict the effect of known biases in the LLNL 2-D model chemistry. As discussed in section 3.1, modeled OH and Cl mixing ratios may be too low in the lower stratosphere by about 20% and up to 25%, respectively. If we were to increase Cl mixing ratios in the model by 25%, and thus increase f_{Cl}, the model would produce heavier isotopic compositions for both carbon and hydrogen, since the Cl KIEs are the largest of the three for both isotopologues. Using Rayleigh estimates, this increase in f_{Cl} would increase the predicted $\delta^{13}C$-CH_4 by up to 3‰ at 700 ppbv CH_4, which is in the right direction to improve the agreement between model results and observations, but it would simultaneously increase the discrepancy between the observations and the hydrogen isotopic composition by up to 11‰. If we were to increase f_{OH} by 25%, the predicted carbon isotopic composition would be lighter by up to 10‰, which would clearly increase the discrepancy between model results and observations. If both the OH and Cl radical abundances were increased, $f_{O(1D)}$ would decrease. For $\delta^{13}C$-CH_4, the Rayleigh estimate indicates that increasing both OH and Cl by 25% (and thus decreasing $f_{O(1D)}$) would yield results heavier by ~0.5‰, which helps to reduce the discrepancy with observations. However, these same changes would make the model predictions for δD-CH_4 heavier by up to 8‰, which would increase the discrepancy with observations. Thus, these changes to OH and Cl abundances, which go in the direction of the LLNL 2-D model known biases, do not appear to simultaneously reduce the discrepancies for both isotope:tracer relationships. Finally, an increase in $f_{O(1D)}$ alone would yield lighter predicted isotopic compositions for carbon and hydrogen scenarios by as much as 0.5‰ and 10‰ respectively. This latter change would decrease the agreement for $\delta^{13}C$-CH_4 only slightly, and greatly increase the agreement for δD-CH_4, a combination which might be acceptable in an attempt to improve the overall agreement. However, increasing $f_{O(1D)}$ does not go in the direction of the known model biases, given the discussion in section 3.1 which suggested that modeled $O(^1D)$ mixing ratios are actually slightly high in the lower stratosphere, while OH and Cl are too low. Furthermore, the new *Ravishankara et al.* [2002] quenching rate coefficient for $O(^1D)$ with N_2 would yield a lower value for $f_{O(1D)}$ than the JPL recommendation used in the model. Overall, these estimates do not rule out other possible chemistry errors as a source of the model-observation discrepancies at low CH_4 mixing ratios for both isotopes. However, these Rayleigh calculations provide estimated upper limits which show that the known biases of the LLNL 2-D model oxidants cannot simultaneously resolve the discrepancies between observations and predicted isotopic compositions for both $\delta^{13}C$-CH_4 and δD-CH_4.

[43] It is also possible that inaccuracies in overall model transport may contribute to the model-observation discrepancies. In general, model transport and mixing which are too weak would result in predicted values for isotopic compositions which are heavier than the observations while transport and mixing which are too strong would result in lighter values. Thus, we expect that an increase in model transport and mixing would result in lighter δD-CH_4 values and bring the D_S1 model results (as well as those for D_S3 and D_S4) closer to the ER-2 observations. However, predicted isotopic compositions for $\delta^{13}C$-CH_4 are too light for the same latitudes and months, so stronger transport would increase the discrepancy between $\delta^{13}C$-CH_4 model results and ER-2 observations. Thus, altering transport alone to better reproduce one observed isotope:tracer relationship would likely result in further disagreement in the other isotope:tracer relationship. In summary, then, the analysis in this section suggests that some combination of changes in chemistry, transport, and/or KIEs may be needed to resolve the model:measurement discrepancies, which is discussed further in the following section.

4.5. Implications of Model-Measurement Comparisons and Model Sensitivities for KIEs

[44] Given the limitations of uncertainties in model chemistry and transport discussed in the preceding section, we now address the question as to whether discrepancies between experimentally determined KIEs can be resolved from the combination of the $\delta^{13}C$-CH_4 and δD-CH_4 observations. As we outline below, only in the case of the carbon KIE for $CH_4 + O(^1D)$ do the observations favor one KIE over another. For all others we examine the sensitivity of the

modeled isotopic compositions to each experimental KIE for future stratospheric and tropospheric applications.

[45] For the $\delta^{13}C$:CH_4 model-measurement comparison, results from Scenario C_S1 (with an OH KIE of 1.0054) and Scenario C_S3 (with an OH KIE of 1.0039) demonstrate that this small difference in OH KIEs yields very little difference in predicted $\delta^{13}C$:CH_4 relationships in the stratosphere. Thus, additional experimental work to resolve the discrepancy between these values for the carbon OH KIE is not needed for stratospheric applications, but is still important for tropospheric studies [e.g., *McCarthy et al.*, 2001]. Likewise, the small difference between the *Tyler et al.* [2000] and *Saueressig et al.* [1996] Cl KIEs cannot be resolved using the ER-2 observations since the predicted difference between C_S1 and CS_4 is likely smaller than uncertainties in model chemistry and transport. In either case, however, the carbon Cl KIE appears to be reasonably well constrained compared to the other KIEs for both stratospheric and tropospheric applications. In contrast, the order of magnitude difference in the $O(^1D)$ KIEs of 1.013 (Scenario C_S1) and 1.001 (Scenario C_S2) results in differences in stratospheric $\delta^{13}C$-CH_4 of ~2‰ or larger at low CH_4 mixing ratios. This difference is larger than the model uncertainties in radical abundances would suggest (see section 4.3, as well as *Wang et al.* [2002]), particularly when the double constraint from the δD-CH_4 observations is taken into account. Using the larger $O(^1D)$ KIE of 1.013 results in a heavier $\delta^{13}C$:CH_4 relationship that is both much closer to the ER-2 observations than using an $O(^1D)$ KIE of 1.001 and has a more realistic curvature given both the ER-2 and the Sugawara balloon observations. These results suggest that the $O(^1D)$ KIE is indeed as large as 1.013. This conclusion is similar to that reached using results from the Harvard 2-D model in a comparison with the balloon $\delta^{13}C$-CH_4 observations [*Wang et al.*, 2002], despite the large differences in transport and chemistry between these two models (see sections 3.1 and 3.2). In order to refine model predictions of the $\delta^{13}C$-CH_4 of stratospheric methane, additional experimental work measuring the KIE for $O(^1D) + CH_4$ would therefore be valuable.

[46] For the δD:CH_4 model-measurement comparison, we are unable to conclusively differentiate among possible values for individual hydrogen experimental KIEs. To within the combined potential uncertainties in model transport and model chemistry, all of the hydrogen KIE model scenarios except D_S1 predict the observations reasonably well. A comparison of all scenarios at $CH_4 < 1200$ ppbv indicates that any one or more of the KIEs could contribute to the discrepancy between D_S1 and observations. Lowering the Gierczak OH KIE by its 1σ uncertainty, the Saueressig Cl KIE by its 2σ uncertainty, or changing the Saueressig $O(^1D)$ KIE to unity all bring these scenarios (D_S3, D_S4, and D_S2) significantly closer to observations. Thus, the uncertainties in each experimental value for the hydrogen KIEs are too large to determine which one(s) may be most likely to contribute to the discrepancy between D_S1 and the observations. Although the DeMore OH KIE in Scenario D_S5 results in a δD:CH_4 relationship that is systematically closer to the observations for $CH_4 <$ 1300 ppbv, uncertainties in model chemistry and transport could erroneously contribute to at least some of this agreement.

[47] Additionally, all model scenarios predict δD-CH_4 values that are heavier than the observations by ~10‰ between CH_4 mixing ratios of ~1200 and 1650 ppbv despite the fact that the model is prescribed to match the δD:CH_4 relationship for air entering the stratosphere (i.e., at 1720 ppbv CH_4). Within the context of the excellent agreement for $\delta^{13}C$-CH_4 at CH_4 mixing ratios >1200 ppbv, the discrepancy at similar mixing ratios for δD-CH_4 suggests that the OH KIE may be the most likely candidate for reduction. Since CH_4 oxidation in the lower stratosphere is dominated by reaction with OH, it is possible that the magnitudes of the Gierczak and DeMore OH KIEs used in the model may be too large at the low temperatures in the lower stratosphere. However, there are other possible explanations for the discrepancy. First, the Cl KIEs could also be too high at low temperatures, even though Cl is responsible for a smaller fraction of CH_4 oxidation in the lower stratosphere. Second, model transport may be too weak in the lower stratosphere, and thus would not adequately attenuate the α_{KIE} to match the α_{app}. However, increasing model transport may also attenuate the predicted value of the carbon isotopic composition, which would reduce model-measurement agreement. Finally, a combination of inaccuracies in modeled radical abundances and model transport might also be responsible for the model-observation discrepancies at high and low CH_4 mixing ratios for $\delta^{13}C$-CH_4 and δD-CH_4. Regardless of the factor(s) responsible for the discrepancy, however, we cannot reconcile the D_S1 KIEs with observations using known biases in the LLNL 2-D model without causing increased discrepancies for the $\delta^{13}C$-CH_4 scenarios. The results of this analysis therefore suggest that additional experimental work on the hydrogen KIEs for CH_4 may be needed for both tropospheric and stratospheric applications. Low temperature KIE studies in particular would aid future stratospheric modeling work. In addition, the discrepancy between the Gierczak and DeMore values for the OH KIE at tropospheric temperatures results in a large difference in α_{KIE}^{H}'s in the troposphere, as seen by comparing Figures 10a and 10b. The discrepancy in these two values will lead to significant differences in predicted δD-CH_4 in the free troposphere.

4.6. Model-Model Comparisons of $\delta^{13}C$:CH_4 and δD:CH_4 as a Diagnostic for Integrated Chemistry and Transport

[48] The analyses here also suggest that intercomparisons of results from different models with stratospheric observations of the $\delta^{13}C$:CH_4 and δD:CH_4 relationships may be useful as a new diagnostic of integrated chemistry and transport in models. For example, the majority of the published CH_4 isotope modeling studies focused on the altitude and latitude distribution of stratospheric $\delta^{13}C$-CH_4 [*Gupta et al.*, 1996; *Bergamaschi et al.*, 1996; *Tyler et al.*, 1999]. However, by focusing on isotope:tracer relationships, a comparison of the LLNL 2-D and Harvard 2-D model [*Wang et al.*, 2002] reveals significant differences between them which are difficult to discern from contour plots alone. The LLNL 2-D model simulated the observed ER-2 $\delta^{13}C$:CH_4 relationship relatively closely for C_S1, to within 0.2‰ at 900 ppbv. However, the Harvard 2-D model is 1 to 2‰ lower than the LLNL 2-D model using the same KIEs for comparable latitudes [*Wang et al.*, 2002]. This difference is consistent with Cl abundances in the Harvard

2-D model that are lower than both observations and the LLNL 2-D model predictions by a factor of 2 to 3 in the lower stratosphere. In addition, the new ER-2 observations allow comparisons of the δD:$\delta^{13}C$ relationship to be used as an additional constraint on integrated model chemistry and transport while minimizing the need to select specific model latitudes for comparison, as discussed in section 4.3. While assessing absolute agreement between model results and stratospheric observations will require additional laboratory measurements to resolve discrepancies among the experimentally determined values for the KIEs, the relative agreement between model results for different models using the same set of KIEs can be used to reveal important differences in integrated Cl, OH, and $O(^1D)$ abundances and in transport characteristics between the models. These differences could then be further examined against additional tracers that are also sensitive to OH, Cl, or $O(^1D)$ mixing ratios.

5. Summary and Conclusions

[49] By incorporating sets of isotope-specific rate coefficients into the LLNL 2-D model, the carbon and hydrogen isotopic compositions of stratospheric methane were simulated. By comparing the modeled $\delta^{13}C$:CH_4 and δD:CH_4 relationships with new observations from the ER-2 aircraft [*Rice et al.*, 2003] and older balloon measurements [*Sugawara et al.*, 1997], we analyzed various model sensitivities to different sets of experimentally determined KIEs. Differences between model results and the observations could be due to uncertainties in the KIEs, errors in model chemistry or transport, measurement errors, or some combination of these factors. We estimated different possible sources of model error using observations of CH_4 mixing ratios, CH_4:N_2O correlations, radical abundances, and mean ages, and comparisons of both $\delta^{13}C$-CH_4 and δD-CH_4. Model results clearly showed that the apparent fractionation factors increase as CH_4 mixing ratios decrease due to changes in the fraction of CH_4 oxidized by each of the oxidants OH, Cl, and $O(^1D)$, as hypothesized in *Rice et al.* [2003]. The 2-D model also demonstrated the importance of transport in determining isotopic compositions, particularly in the contrast between the tropics and the extratropics.

[50] We also assessed whether the stratospheric observations could be used to gain insight into discrepancies between experimental values for the various hydrogen and carbon KIEs. In the case of the order of magnitude difference between carbon KIEs for the reaction of CH_4 with $O(^1D)$, our analysis strongly suggests that the larger KIE of 1.013 is required to reproduce the observed $\delta^{13}C$:CH_4 relationship. In the analysis of model scenarios comparing all other KIEs, it was difficult to distinguish between uncertainties in experimental values for KIEs and the estimated effects of model uncertainties. For example, discrepancies between the experimental values for the carbon KIEs of OH are too small to alter stratospheric $\delta^{13}C$-CH_4 beyond uncertainties in model chemistry and transport. For the hydrogen KIEs, model-measurement comparisons at low CH_4 mixing ratios may indicate that any one or more of the KIEs is too large. At high CH_4 mixing ratios, model results for δD-CH_4 are suggestive that one or both of the hydrogen KIEs for reaction with OH and Cl are too large at low stratospheric temperatures. However, the disagreement between the model results and observations for all hydrogen KIE scenarios could also be due to difficulties in simulating stratospheric transport or radical abundances in the lower stratosphere.

[51] Finally, the comparisons of 2-D model results with stratospheric observations presented here point to several specific field, modeling, and laboratory studies that should be pursued. Of high importance is the acquisition of high-precision measurements of $\delta^{13}C$-CH_4 and δD-CH_4 in the tropics that extend to high altitudes (>30 km). Such tropical observations would provide important new constraints on the underlying carbon and hydrogen KIEs and would allow a significant extension of the analysis presented here, as well as providing new diagnostics for model-model comparisons. Future modeling work suggested by this study, in addition to pursuing the model-model intercomparisons noted above, might also include using a least-squares method of determining the set of KIEs required to reproduce observed $\delta^{13}C$-CH_4:CH_4, δD-CH_4:CH_4, and δD-CH_4:$\delta^{13}C$-CH_4 relationships at mid-latitudes with a simple 1D model that uses transport coefficients known to reproduce correlations between other long-lived tracer correlations, such as the correlation between CO_2 and N_2O [e.g., *Wofsy et al.*, 1994]; sensitivities to values for KIEs and prescribed radical concentrations could be more rapidly evaluated in this way rather than full implementation of different sets of KIEs in a 2-D model. Additional laboratory studies of the magnitudes of the KIEs and their temperature dependences are also of high importance. These new laboratory measurements may help to resolve current discrepancies among experimental values that cannot be distinguished in the model study presented here, and will ultimately allow the stratospheric isotope observations to serve as diagnostics of model chemistry and transport in the future.

[52] **Acknowledgments.** We thank Stephen Donnelly, Rich Lueb, Sue Schauffler, and Verity Stroud for support of the ER-2 whole air sampling and methane measurements and Michael Bender for helpful discussions. We gratefully acknowledge support through grants to UC Berkeley from the NASA Atmospheric Chemistry, Modeling and Analysis Program (NAG-1-2191 and NAG-1-02083), the NASA Upper Atmosphere Research Program (NAG-2-1483), and the NSF Atmospheric Chemistry Program (ATM-9901463) and for a Packard Foundation Fellowship in Science and Engineering for K.A.B.; to UC Irvine from the NASA Earth System Science Fellowship for A.R. (NAGTA5-50226), the NASA EOS Validation award (NAG5-9955), NASA Carbon Cycle Science award (NGT5-30409), an NSF major research instrumentation award (ATM-9871077), and a Keck Foundation instrument grant to UC Irvine; and to NCAR from the NASA Upper Atmosphere Research Program and the National Science Foundation. Portions of this work were also performed under the auspices of the U.S. Department of Energy by the University of California, Lawrence Livermore National Laboratory, under contract W-7405-Eng-48.

References

Allan, W., M. R. Manning, K. R. Lassey, D. C. Lowe, and A. J. Gomez, Modeling the variation of $\delta^{13}C$ in atmospheric methane: Phase ellipses and the kinetic isotope effect, *Global Biogeochem. Cycles*, *15*, 467–481, 2001.

Bergamaschi, P., C. Brühl, C. A. M. Brenninkmeijer, G. Saueressig, J. N. Crowley, J. U. Grooß, H. Fischer, and P. J. Crutzen, Implications of the large C KIE in CH_4 + Cl for stratospheric CH_4, *Geophys. Res. Lett.*, *23*, 2227–2230, 1996.

Boone, G. D., F. Aygin, D. J. Robichaud, F. Tao, and S. A. Hewitt, Rate constants for the reaction of Cl atoms with deuterated methanes: Experiment and theory, *J. Phys. Chem.*, *105*, 1456–1464, 2001.

Braunlich, M., O. Aballain, T. Marik, P. Jockel, C. A. M. Brenninkmeijer, J. Chappellaz, J. Barnola, R. Mulvaney, and W. T. Sturges, Changes in the global atmospheric methane budget over the last decades inferred from ^{13}C and D isotopic analysis of Antarctic firn air, *J. Geophys. Res.*, *106*, 20,465–20,481, 2001.

Brenninkmeijer, C. A. M., D. C. Lowe, M. R. Manning, R. J. Sparks, and P. F. J. Vanvelthoven, The ^{13}C, ^{14}C, and ^{18}O isotopic composition of CO, CH_4, and CO_2 in the higher southern latitudes lower stratosphere, *J. Geophys. Res.*, *100*, 26,163–26,172, 1995.

Cantrell, C. A., R. E. Shetter, A. H. McDaniel, J. G. Calvert, J. A. Davidson, D. C. Lowe, S. C. Tyler, R. J. Cicerone, and J. P. Greenberg, Carbon KIE in the oxidation of CH_4 by OH, *J. Geophys. Res.*, *95*, 22,455–22,462, 1990.

Corchado, J. C., D. G. Truhlar, and J. Espinosa-Garcia, Potential energy surface, thermal, and state-selected rate coefficients, and kinetic isotope effects for $Cl + CH_4 \rightarrow HCl+CH_3$, *J. Phys. Chem.*, *112*, 9375–9389, 2000.

Crowley, J. N., G. Saueressig, P. Bergamaschi, H. Fischer, and G. W. Harris, Carbon KIE in the reaction CH_4 + Cl, *Chem. Phys. Lett.*, *303*, 268–274, 1999.

Davidson, J. A., C. A. Cantrell, S. C. Tyler, R. E. Shetter, R. J. Cicerone, and J. G. Calvert, Carbon KIE in the reaction of CH_4 with HO, *J. Geophys. Res.*, *92*, 2195–2199, 1987.

DeMore, W. B., Rate constant ratio for the reactions of OH with CH_3D and CH_4, *J. Phys. Chem.*, *97*, 8564–8566, 1993.

DeMore, W. B., S. P. Sander, D. M. Golden, R. F. Hampson, M. J. Kurylo, C. J. Howard, A. R. Ravishankara, C. E. Kolb, and M. J. Molina, Chemical kinetics and photochemical data for use in stratospheric modeling—Evaluation 12, *JPL Publ.*, *97-4*, 1997.

DeMore, W. B., et al., Chemical kinetics and photochemical data for use in stratospheric modeling—Evaluation 13, *JPL Publ*, *00-3*, 2000.

Dlugokencky, E. J., B. P. Walter, K. A. Masarie, P. M. Lang, and E. S. Kasischke, Measurements of an anomalous global methane increase during 1998, *Geophys. Res. Lett.*, *28*, 499–502, 2001.

Eluszkiewicz, J., R. S. Hemler, J. D. Mahlman, L. Bruhwiler, and L. L. Takacs, Sensitivity of age-of-air calculations to the choice of advection scheme, *J. Atmos. Sci.*, *57*(19), 3185–3201, 2000.

Espinosa-Garcia, J., and J. C. Corchado, Potential energy surface for a seven-atom reaction: Thermal rate constants and kinetic isotope effects for CH_4 + OH, *J. Phys. Chem.*, *112*, 5731–5739, 2000.

Flocke, F., et al., An examination of chemistry and transport processes in the tropical lower stratosphere using observations of long-lived and short-lived compounds obtained during STRAT and POLARIS, *J. Geophys. Res.*, *104*, 26,625–26,642, 1999.

Fung, I., J. John, J. Lerner, E. Matthews, M. Prather, L. P. Steele, and P. J. Fraser, Three-dimensional model synthesis of the global CH_4 cycle, *J. Geophys. Res.*, *96*, 13,033–13,065, 1991.

Gierczak, T., R. K. Talukdar, S. C. Herndon, G. L. Vaghjiani, and A. R. Ravishankara, Rate coefficients for the reactions of hydroxyl radicals with methane and deuterated methanes, *J. Phys. Chem.*, *101*, 3125–3134, 1997.

Gordon, S., and W. A. Mulac, Reaction of OH(X2-PI) radical produced by pulse radiolysis of water-vapor, *Int. J. Chem. Kinet.*, *7*(1), 289–299, 1975.

Gupta, M. L., S. Tyler, and R. J. Cicerone, Modeling atmospheric $\delta^{13}CH_4$ and the causes of recent changes in atmospheric CH_4 amounts, *J. Geophys. Res.*, *101*, 22,923–22,932, 1996.

Gupta, M. L., M. P. McGrath, R. J. Cicerone, F. S. Rowland, and M. Wolfsberg, C-12/C-13 kinetic isotope effects in the reactions with OH and Cl, *Geophys. Res. Lett.*, *24*, 2761–2764, 1997.

Hall, T. M., D. W. Waugh, K. A. Boering, and R. A. Plumb, Evaluation of transport in stratospheric models, *J. Geophys. Res.*, *104*, 18,815–18,839, 1999.

Hanisco, T. F., et al., Sources, sinks, and the distribution of OH in the lower stratosphere, *J. Phys. Chem.*, *105*, 1543–1553, 2001.

Hein, R., and P. J. Crutzen, An inverse modeling approach to investigate the global atmospheric CH_4 cycle, *Global Biogeochem. Cycles*, *11*, 43–76, 1997.

Herman, R. L., et al., Tropical entrainment timescales inferred from stratospheric N_2O and CH_4 observations, *Geophys. Res. Lett.*, *25*(15), 2781–2784, 1998.

Houweling, S., T. Kaminski, F. Dentener, J. Lelieveld, and M. Heimann, Inverse modeling of methane sources and sinks using the adjunct of a global transport model, *J. Geophys. Res.*, *104*, 26,137–26,160, 1999.

Hurst, D. F., et al., Closure of the total hydrogen budget of the northern extratropical lower stratosphere, *J. Geophys. Res.*, *104*, 8191–8200, 1999.

Irion, F. W., et al., Stratospheric observations of CH_3D and HDO from ATMOS infrared solar spectra: Enrichments of deuterium in methane and implications for HD, *Geophys. Res. Lett.*, *23*, 2381–2384, 1996.

Kaye, J. A., Mechanisms and observations for isotopic fractionation of molecular species in planetary atmospheres, *Rev. Geophys.*, *25*, 1609–1658, 1987.

Kinnison, D. E., K. E. Grant, P. S. Connell, D. A. Rotman, and D. J. Wuebbles, The chemical and radiative effects of the Mt. Pinatubo eruption, *J. Geophys. Res.*, *99*, 25,705–25,731, 1994.

Lasaga, A. C., and G. V. Gibbs, Ab initio studies of the kinetic isotope effect of the CH_4 + OH atmospheric reaction, *Geophys. Res. Lett.*, *18*(7), 1217–1220, 1991.

McCarthy, M. C., P. Connell, and K. A. Boering, Isotopic fractionation of methane in the stratosphere and its effect on free tropospheric isotopic compositions, *Geophys. Res. Lett.*, *28*, 3567–3570, 2001.

Melissas, V. S., and D. G. Truhlar, Deuterium and carbon-13 kinetic isotope effects for the reaction of OH with CH_4, *J. Chem. Phys.*, *99*(5), 3542–3552, 1993.

Michelsen, H. A., Carbon and hydrogen kinetic isotope effects for the reaction of $Cl + CH_4$: Consolidating chemical kinetics and molecular dynamics measurements, *J. Geophys. Res.*, *106*, 12,267–12,274, 2001.

Michelsen, H. A., et al., Stratospheric chlorine partitioning: Constraints from shuttle-borne measurements of [HCl], [$ClNO_3$], and [ClO], *Geophys. Res. Lett.*, *23*, 2361–2364, 1996.

Michelsen, H. A., G. L. Manney, M. R. Gunson, C. P. Rinsland, and R. Zander, Correlations of stratospheric abundance of CH_4 and N_2O derived from ATMOS measurements, *Geophys. Res. Lett.*, *25*(15), 2777–2780, 1998.

Park, J. H., M. K. W. Ko, C. H. Jackman, R. A. Plumb, J. A. Kaye, and K. H. Sage, Models and measurements intercomparison II, *NASA Tech. Memo., TM-1999-209554*, 1999.

Plumb, R. A., and M. K. W. Ko, Interrelationships between mixing ratios of long-lived stratospheric constituents, *J. Geophys. Res.*, *97*, 10,145–10,156, 1992.

Plumb, R. A., D. W. Waugh, and M. P. Chipperfield, The effects of mixing on tracer relationships in the polar vortex, *J. Geophys. Res.*, *105*, 10,047–10,062, 2000.

Quay, P., J. Stutsman, D. Wilbur, A. Snover, E. Dlugokencky, and T. Brown, The isotopic composition of atmospheric CH_4, *Global Biogeochem. Cycles*, *13*, 445–461, 1999.

Randel, W. J., F. Wu, J. M. Russell, A. Roche, and J. W. Waters, Seasonal cycles and QBO variations in stratospheric CH_4 and H_2O observed in UARS HALOE data, *J. Atmos. Sci.*, *55*, 163–185, 1998.

Ravishankara, A. R., E. J. Dunlea, M. A. Blitz, T. J. Dillon, D. E. Heard, M. J. Pilling, R. S. Strekowski, J. M. Nicovich, and P. H. Wine, Redetermination of the rate coefficient for the reaction of $O(^1D)$ with N_2, *Geophys. Res. Lett.*, *29*(15), doi:10.1029/2002GL014850, 2002.

Rex, M., et al., Subsidence, mixing, and denitrification of Arctic polar vortex air measured during POLARIS, *J. Geophys. Res.*, *104*, 26,611–26,623, 1999.

Rice, A. L., A. A. Gotoh, H. O. Ajie, and S. C. Tyler, High-precision continuous-flow measurement of $\delta^{13}C$ and δD of atmospheric CH_4, *Anal. Chem.*, *73*, 4104–4110, 2001.

Rice, A. L., S. C. Tyler, M. C. McCarthy, K. A. Boering, and E. Atlas, Carbon and hydrogen isotopic compositions of stratospheric methane: 1. High-precision observations from the NASA ER-2 aircraft, *J. Geophys. Res.*, *108*, doi:10.1029/2002JD003042, in press, 2003.

Roberto-Neto, O., E. L. Coitino, and D. G. Truhlar, Direct dynamics calculations of deuterium and carbon-13 kinetic isotope effects for the reaction $Cl + CH_4$, *J. Phys. Chem.*, *102*, 4568–4578, 1998.

Roehl, C. M., S. A. Nizkorodov, H. Zhang, G. A. Blake, and P. O. Wennberg, Photodissociation of peroxynitric acid in the near-IR, *J. Phys. Chem.*, *106*, 3766–3772, 2002.

Rust, F., and C. M. Stevens, Carbon kinetic isotope effect in the oxidation of methane by hydroxyl radical, *Int. J. Chem. Kinet.*, *12*, 371–377, 1980.

Saueressig, G., P. Bergamaschi, J. N. Crowley, and H. Fischer, Carbon KIE in the reaction of CH_4 with Cl atoms, *Geophys. Res. Lett.*, *22*, 1225–1228, 1995.

Saueressig, G., P. Bergamaschi, J. N. Crowley, H. Fischer, and G. W. Harris, D/H kinetic isotope effect in the reaction CH_4 + Cl, *Geophys. Res. Lett.*, *23*, 3619–3622, 1996.

Saueressig, G., J. N. Crowley, P. Bergamaschi, C. Brühl, C. A. M. Brenninkmeijer, and H. Fischer, Carbon-13 and D kinetic isotope effects in the reactions of CH_4 with $O(^1D)$ and OH: New laboratory measurements and their implications for the isotopic composition of stratospheric methane, *J. Geophys. Res.*, *106*, 23,127–23,138, 2001.

Shine, K. P., Y. Fouquart, V. Ramaswamy, S. Solomon, and J. Srinivasan, Radiative forcing of climate change, in *Climate Change 1995: The Science of Climate Change*, *Scientific Assessment Work Group I of Intergovernmental Panel on Climate Change*, pp. 108–118, Cambridge Univ. Press, New York, 1996.

Simpson, I. J., T.-Y. Chen, D. R. Blake, and F. S. Rowland, Implications of the recent fluctuations in the growth rate of tropospheric methane, *Geophys. Res. Lett.*, *29*(10), doi:10.1029/2001GL014521, 2002.

Sugawara, S., T. Nakazawa, Y. Shirakawa, K. Kawamura, S. Aoki, T. Machida, and H. Honda, Vertical profile of the carbon isotopic ratio of stratospheric methane over Japan, *Geophys. Res. Lett.*, *24*, 2989–2992, 1997.

Tanaka, N., Y. Xiao, and A. C. Lasaga, Ab initio study on carbon kinetic isotope effect (KIE) in the reaction of CH_4 + Cl, *J. Atmos. Chem.*, *23*, 37–49, 1996.

Tyler, S. C., H. O. Ajie, M. L. Gupta, R. J. Cicerone, D. R. Blake, and E. Dlugokencky, A comparison of surface level and free tropospheric $\delta^{13}CH_4$, *J. Geophys. Res.*, *104*, 13,895–13,910, 1999.

Tyler, S. C., H. O. Ajie, A. L. Rice, R. J. Cicerone, and E. C. Tuazon, Experimentally determined KIEs in the reaction of CH_4 with Cl, *Geophys. Res. Lett.*, *27*, 1715–1718, 2000.

Wahlen, M., B. Deck, R. Henry, A. Shemesh, R. Fairbanks, W. Broecker, H. Weyer, B. Marino, and J. Logan, Profiles of $\delta^{13}C$ and δD of CH_4 from the lower stratosphere, *Eos Trans. AGU*, *70*, 1017, 1989.

Wallington, T. J., and M. D. Hurley, A kinetic study of the reaction of chlorine atoms with CF_3CHCl2, CF_3CH_2F, $CFCl_2CH_3$, CF_2ClCH_3, CHF_2CH_3, CH_3D, CH_2D_2, CHD_3, CD_4, and CD_3Cl at 295 ± 2 K, *Chem. Phys. Lett.*, *189*, 437–442, 1992.

Wang, J. S., M. B. McElroy, C. M. Spivakovsky, and D. B. A. Jones, On the contribution of anthropogenic Cl to the increase in $\delta^{13}C$ of atmospheric methane, *Global Biogeochem. Cycles*, *16*(3), 1047, doi:10.1029/2001GB001572, 2002.

Waugh, D. W., et al., Mixing of polar vortex air into middle latitudes as revealed by tracer-tracer scatterplots, *J. Geophys. Res.*, *102*, 13,119–13,134, 1997.

Wofsy, S. C., K. A. Boering, B. C. Daube, M. B. McElroy, M. Loewenstein, J. R. Podolske, J. W. Elkins, G. S. Dutton, and D. W. Fahey, Vertical transport rates in the stratosphere in 1993 from observations of CO_2, N_2O, and CH_4, *Geophys. Res. Lett.*, *21*, 2571–2574, 1994.

World Meteorological Organization (WMO), Scientific assessment of O_3 depletion: 1998, *Proj. Rep. 44*, U. N. Environ. Programme, Geneva, 1999.

E. Atlas, Atmospheric Chemistry Division, National Center for Atmospheric Research, Boulder, CO 80305, USA.

K. A. Boering and M. C. McCarthy, Department of Chemistry, University of California, Berkeley, CA 94720-1460, USA. (boering@cchem.berkeley.edu)

P. Connell, Atmospheric Sciences Division, Lawrence Livermore National Laboratory, Livermore, CA 94550, USA.

A. L. Rice, Joint Institute for the Study of the Atmosphere and Ocean, University of Washington, Seattle, WA 98195, USA.

S. C. Tyler, Department of Earth System Science, University of California, Irvine, CA 92717, USA.